الجمهورية الجزائرية الديمقراطية الشعبية

LA REPUBLIQUE ALGERIENNE DEMOCRATIQUE ET POPULAIRE
THE DEMOCRATIC AND POPULAR REPUBLIC OF ALGERIA

وزارة التعليم العالي والبحث العلمي

Ministère de l'Enseignement Supérieur et de la Recherche Scientifique
Ministry of Higher Education and Scientific Research

Saad Dahlab University Blida 1

Institute of Aeronautics and Space Studies

Spatial Studies Department

Final Year Dissertation

For The Purpose of Obtaining A

Master's Degree in Aeronautics

Option: **Space Telecommunications**

THEME

Modeling of a Triple Junction Solar cell

Defended by:

- **Mr. Bennouar Adnane**
- **Mr. Bouzourine Abderrahmane**

Supervised by:

- **Dr. Benkercha Rabah**
- **Dr. Tahraoui Sofiane**
- **Dr. Teffah Khaled**

Sustained in front of the jury consists of :

Pr. Lagha Mohand	*Professeur*	*Président*
Dr. Azmedroub Boussad	*MCB*	*Examinateur*

Promotion : 2022 / 2023

ACKNOWLEDGMENTS

In the name of Allah, the Most Merciful, the Most Compassionate, we begin by expressing our heartfelt gratitude to the Almighty for His abundant blessings, guidance, and unwavering support throughout our journey.

We would like to express our deepest appreciation to Dr.BENKERCHA RABAH and Dr.TAHRAOUI SOFIANE , our supervisors and mentors. Your wisdom, patience, and unwavering belief in our potential have been instrumental in our growth and success. Your guidance and constant encouragement have helped us navigate through the challenges and push ourselves beyond our limits. We are truly grateful for the opportunity to learn from you and for the trust you have placed in us.

We would like to express our heartfelt appreciation to Dr. TEFFAH KHALED for his invaluable role as our mentor during our time at The Algerian Space Agency (ASAL), which I would like to express my gratitude for its friendly and welcoming work environment, my future endeavors in the field of space exploration and technology will unquestionably be influenced by the knowledge and experience gained during this period and it would be a privilege to maintain contact with the organization and contribute to its future projects wholeheartedly. Dr.TEFFAH guidance and assistance were instrumental in our growth and development, and we are immensely grateful for his unwavering support, his presence has made a profound impact on our experience, and we are truly honored to have had him by our side.

Lastly, we want to express our sincere appreciation to all our friends, colleagues, and well-wishers who have supported us along this challenging journey. Your words of encouragement, belief in our abilities, and acts of kindness have touched our hearts and motivated us to persevere.

May Allah bless each and every one of you for your invaluable contributions and may our journey serve as a reminder that with determination, support, and gratitude, we can overcome any obstacles that come our way.

Bennouar Adnane & Bouzourine Abderrahmane

TABLE OF CONTENTS

LIST OF TABLES

LIST OF FIGURES

LIST OF ABREVIATIONS

LEO: **L**ow **E**arth **O**rbit

MEO: **M**edium **E**arth **O**rbit

GEO: **G**eostationary **O**rbit

PV: **P**hotovoltaic

c-Si: **C**rystalline **S**ilicon

mc-Si: **M**onolycrystalline **S**ilicon

pc-Si: **P**olycrystalline **S**ilicon

BIPV: **B**uilding **I**ntegrated **P**hotovoltaics

a-Si: **A**morphous **S**ilicon

µc-Si: **M**icro-**c**rystalline **S**ilicon

CdTe: **C**admium **T**elluride

CPV: **C**oncentrator **P**hotovoltaics

OPV: **O**rganic **P**hotovoltaics

Isc: **S**hort-**c**ircuit **C**urrent

Voc: **O**pen-**c**ircuit Current

MPP: **M**aximum **P**ower **P**oint

Vmp: **M**aximum **P**ower **V**oltage

Imp: **M**aximum **P**ower **C**urrent

STC: **S**tandard **T**est **C**onditions

FF: **F**ill **F**actor

PERC: **P**assivated **E**mitter **R**ear **C**ell

PERT: **P**assivated **E**mitter **R**ear **T**otally diffused

PERL: **P**assivated **E**mitter **R**ear **L**ocally diffused

IBC: **I**ntegrated **B**ack **C**ontact

HIT: **H**eterojunction

HBC: **H**eterojunction **B**ack **C**ontact

Si/Ge : **S**ilicon/**Ge**rmanium

MBE: **M**olecular **B**eam **E**pitaxy

HRXRD: **H**igh **R**esolution **X**-**R**ay **D**iffraction

ARC: **A**nti **R**eflective **C**oatings

PECVD: **P**lasma **E**nhanced **C**hemical **V**apor **D**eposition

TJSC: **T**riple **J**unction **S**olar **C**ells

RMSE: **R**oot **M**ean **S**quared **E**rror

ABSTRACT

the PV cell is an indispensable element for The Electrical Power System (EPS) which is responsible for the production and storage of energy needed for subsystems and payloads in a spacecraft. Starting from this, this work enables to discover the properties of a photovoltaic cell. In addition, this study makes it possible to evaluate the performance of the electrical system for a Nano-satellite. In this context, we modeled a PV cell (model the I-V characteristics) using MATLAB software (MATLAB & Simulink) and visualize the different effects that can improve or reduce the capacities of a PV cell. Afterwards, an approach was selected in order to identify the unknown parameters of the PV cell model. Finally, comparison of the model performance with the identified parameters with the actual PV cell data from different studies, which can validate the chosen model in term of being used into different cases.

Keywords : Nanosatellite, PV cells, Triple Junction Solar Cell, Parameters identification

La cellule PV est un élément indispensable pour le système d'alimentation électrique (EPS) qui est responsable de la production et du stockage de l'énergie nécessaire aux sous-systèmes et aux charges utiles d'un vaisseau spatial. Partant de là, ce travail permet de découvrir les propriétés d'une cellule photovoltaïque. De plus, cette étude permet d'évaluer les performances du système électrique d'un Nanosatellite. Dans ce contexte, nous avons modélisé une cellule PV (modéliser les caractéristiques I-V) à l'aide du logiciel MATLAB (MATLAB & Simulink) et visualisé les différents effets qui peuvent améliorer ou réduire les capacités d'une cellule PV. Par la suite, une approche a été sélectionnée afin d'identifier les paramètres inconnus du modèle de cellule PV. Enfin, comparaison des performances du modèle avec les paramètres identifiés avec les données réelles des cellules PV de différentes études, ce qui peut valider le modèle choisi en termes d'utilisation dans différents cas.

Mots clés : Nanosatellite, Cellules PV, Cellule solaire à triple jonction, Identification des paramètres.

الخلية الكهروضوئية عنصر لا غنى عنه لنظام الطاقة الكهربائية المسؤول عن إنتاج وتخزين الطاقة اللازمة للنظم الفرعية والحمولات في مركبة فضائية. بدءا من هذا، هذا العمل يمكن من اكتشاف خصائص الخلية الكهروضوئية. وبالإضافة إلى ذلك، تتيح هذه الدراسة تقييم أداء النظام الكهربائي للقمر الصناعي صغير الحجم . وفي هذا السياق، قمنا بنموذج خلية كهروضوئية (نموذج الخصائص) باستخدام برامجيات MATLAB وتصورنا التأثيرات المختلفة التي يمكن أن تحسن أو تقلل من قدرات الخلية الكهروضوئية. بعد ذلك ، تم اختيار نهج لتحديد المعلمات غير المعروفة لنموذج الخلية الكهروضوئية. أخيرًا ، مقارنة أداء النموذج بالمعلمات المحددة مع بيانات الخلية الكهروضوئية الفعلية من دراسات مختلفة ، والتي يمكن أن تتحقق من صحة النموذج المختار من حيث استخدامه في حالات مختلفة .

الكلمات الرئيسية: الأقمار الصناعية النانوية ، الخلايا الكهروضوئية ، خلية شمسية ثلاثية التقاطع ، تحديد المعلمات

GENERAL INTRODUCTION

In today's fast progressing world , where every passing second count , Photovoltaic solar cells had being a crucial factor in the development of satellites and space applications , for a satellite to maintain its role and do whatever he's supposed to do , solar cells absorb sun lightning and convert it into power to run the whole system of a spacecraft , whoever , the efficiency of this absorption differ from a cell to another , there are multiple factors that effect this for the worse or for the best , and to maintain a good efficacity , scientists always try to come up with new ideas to help developing the best cell that can transform the highest amount of light into the highest amount of energy with the minimum losses .

The most dominating type of solar cells in space applications are multijunction solar cells and more specifically, Triple junction solar cells, theoretically the more junctions you have the more electricity you can produce but on the other hand the current generated is highly dependent on amount of light exposure.

In Chapter 1, we just announcing the generalities of satellites and solar cells, going through everything that need to be known about it, from types and materials used to design it, to electrical parameters and what effect it most and in what way, the chapter also provides an overview of the subsequent chapters.

In Chapter 2, our primary objective is to provide the readers with a solid foundation of knowledge by explaining the multiple types and equivalent circuits of solar cells from mono-junction to triple junction, but our focus was placed on TJSC where we define all the equations used for the modeling part in chapter 3, and also describe the improvements add to this type of cells over the years from different scientists using different approaches.

Building upon the knowledge given in chapter 2, chapter 3 was about the method of parameter extracting, our focus was to select a method used to extract the parameters then to model a TJSC, next step is testing the method on different types of the same cell with different bandgaps, and compare the results with the data given by the manufacturer of the cell, and finally modeling the TJSC using a physical model (SIMULINK) was our final test to prove the high performance of the chosen method.

At the end of this thesis, a compelling conclusion awaits, summarizing the crux of our work. As we look beyond the confines of this manuscript, we are eager to witness the doors of progress swing open, revealing pathways to future advancements and innovative possibilities in this field.

CHAPTER 1.

GENERALITIES ON AEROSPACE PVSYSTEMES

1.1 Introduction

The sun is an infinite source of energy. The exploitation of this energy has been done since the dawn of time, and the increase in energy needs makes it more and more essential.

On Earth, solar radiation is received intermittently. The sun's rays are obscured by the different layers that make up the atmosphere, as well as by clouds. In addition, the pseudo-spherical geometry of our planet induces a difference in sunshine depending on the location considered. Its movement, at the origin of the day and night phenomenon, halves the perceived solar flux.

In space, solar radiation is not altered, the available energy is therefore nearly ten times greater than that captured by the earth's surface. Moreover, this radiation is constant because it is independent of the seasons of the days and of the weather conditions. Thus, outside the atmosphere, solar energy is as reliable as nuclear energy.

1.2 Satellites

1.2.1 Definition

A satellite is an object in space that orbits or circles around a bigger object. There are two kinds of satellites: natural (such as the moon orbiting the Earth) or artificial (such as the International Space Station orbiting the Earth).

Since the world first listened to Sputnik’s radio beacon, the variety of space applications has multiplied. Satellites serve many military, civil, research, and commercial purposes.

- Militaries use satellites for communications and reconnaissance.
- Governments use satellites to conduct Earth and Space Science research, observe the weather and the environment, and regulate industrial activity.
- Commercial satellites support global communications, provide Earth Observation services, and much more.

1.2.2 History

Artificial satellites did not become a reality until the mid-20th century. The first artificial satellite was Sputnik, a Russian beach-ball-size space probe that lifted off on Oct. 4, 1957. That act shocked much of the western world, as it was believed the Soviets did not have the capability to send satellites into space. Following that feat, on Nov. 3, 1957 the Soviets launched an even more

massive satellite — Sputnik 2 — which carried a dog, Laika. The United States' first satellite was Explorer 1 on Jan. 31, 1958. The satellite was only 2 percent the mass of Sputnik 2, however, at 30 pounds (13 kg). The Sputniks and Explorer 1 became the opening shots in a space race between the United States and the Soviet Union that lasted until at least the late 1960s. The focus on satellites as political tools began to give way to people as both countries sent humans into space in 1961. Later in the decade, however, the aims of both countries began to split. While the United States went on to land people on the moon and create the space shuttle, the Soviet Union constructed the world's first space station, Salyut 1, which launched in 1971. (Other stations followed, such as the United States' Skylab and the Soviet Union's Meir.)

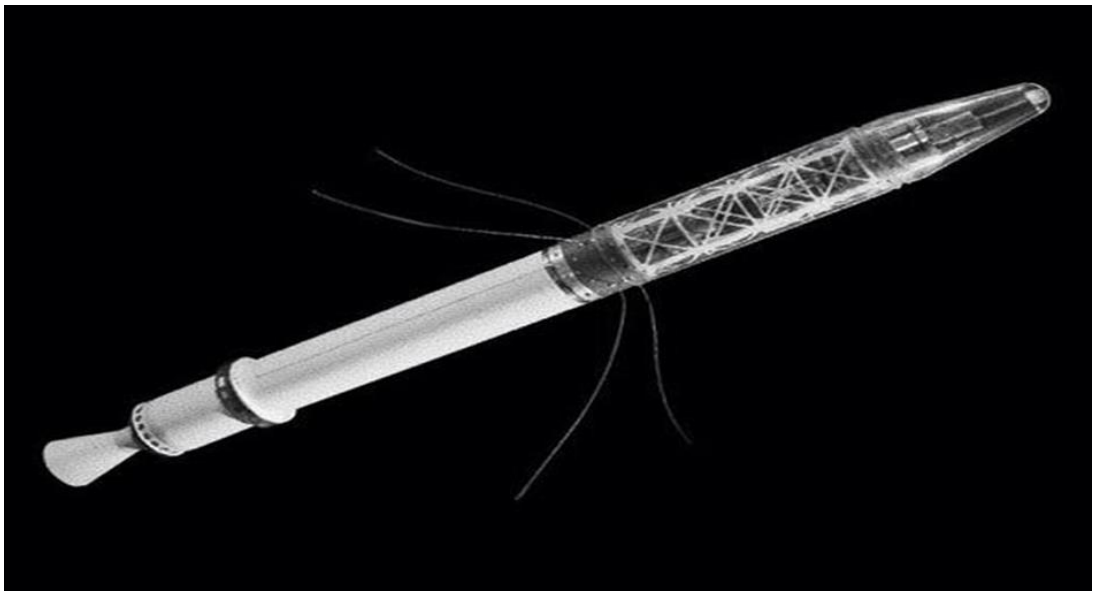

Figure 1-1 Explorer 1 was the first U.S. satellite and the first satellite to carry scientific instruments.

With the decreasing size of computers and other technology, it is now possible to launch considerably smaller satellites into orbit that may serve science, telecommunications, and other purposes. Companies and colleges are increasingly developing "CubeSats," or cube-shaped satellites that often inhabit low-Earth orbit. These can be launched on a rocket alongside a larger payload, or from the International Space Station (ISS) using a mobile launcher. NASA is now exploring sending CubeSats to Mars or the moon Europa (near Jupiter) for future missions, however their inclusion has not been confirmed [1].

1.2.3 Orbits

The diversity of space missions results in a wide variety of orbits. Depending on these missions, the orbits described by the Earth's satellites are organized into three main categories

a) Low-earth-orbit satellites

A low Earth orbit (LEO) is, as the name implies, an orbit that is close to the Earth's surface. It is generally less than 1000 km above Earth, although it can be as low as 160 km above Earth, which is low in comparison to other orbits but still quite far over the Earth's surface. In comparison, most commercial aircraft do not travel at heights much higher than 14 km, therefore even the lowest LEO is more than ten times higher.

Unlike GEO satellites, which must always orbit near the equator, LEO spacecraft do not always have to follow the same path around the Earth - their plane can be inclined. This means that satellites in LEO have more potential paths, which is one of the reasons why LEO is such a popular orbit. Because of its close proximity to Earth, LEO is useful for a variety of reasons. It is the most widely utilized orbit for satellite photography since being close to the surface allows for greater resolution photographs. It is also the orbit utilized by the International Space Station (ISS), as it allows astronauts to travel a shorter distance to and from it. Satellites in this orbit travel at around 7.8 km per second; at this speed, a satellite takes approximately 90 minutes to circle Earth, implying that the ISS travels around Earth approximately 16 times per day. Individual LEO satellites, on the other hand, are less effective for services such as telecommunication since they move so quickly across the sky and therefore demand a lot of effort to track from ground stations.

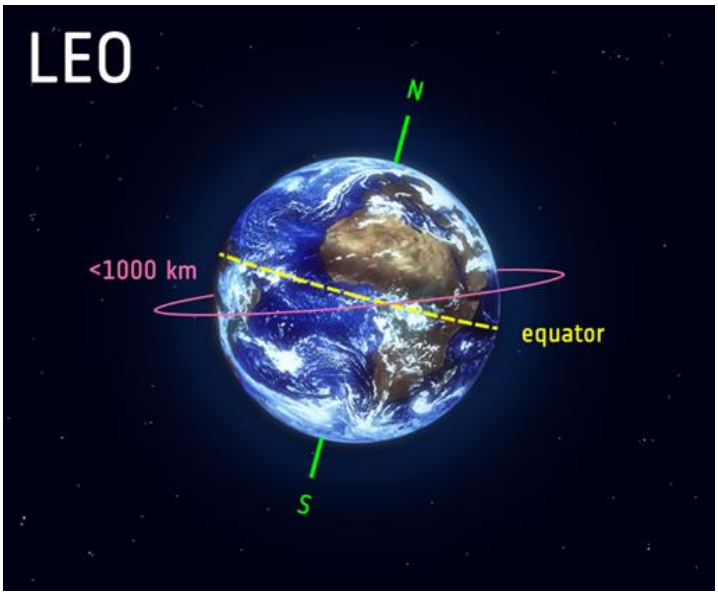

Figure 1-2 Low earth orbit

Instead, communications satellites in low-Earth orbit (LEO) sometimes operate as part of a huge combination, or constellation, of many satellites to provide continuous coverage. To increase coverage,

constellations like this, which consist of numerous of the same or similar satellites, are occasionally launched together to form a 'net' encircling Earth. Working collectively, they can cover enormous parts of the Earth at the same time.

b) Middle-earth-orbit satellites

Medium Earth orbit encompasses a wide range of orbits between LEO and GEO. It is similar to LEO in that it does not need precise trajectories around Earth and is utilized by a wide range of satellites with a wide range of purposes. It is widely utilized by navigation satellites, such as the European Galileo system . Galileo enables navigation communications around Europe and is used for a variety of purposes, including tracking massive jumbo planes and providing instructions to your smartphone. Galileo employs a constellation of many satellites to give coverage across huge areas of the planet at once.

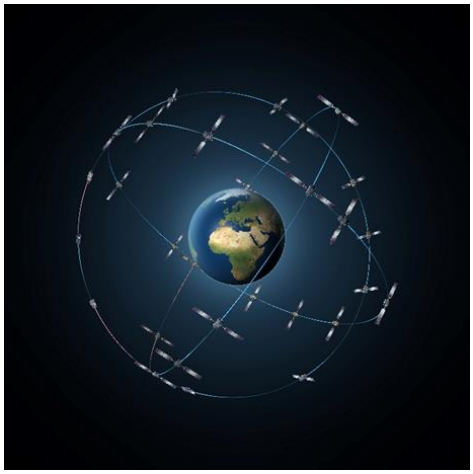

Figure 1-3 Galileo constellation

c) Geostationary orbit satellites

Satellites in geostationary orbit (GEO) circle Earth above the equator from west to east, requiring 23 hours 56 minutes and 4 seconds and traveling at the same pace as Earth. Satellites in GEO appear to be 'stationary' over a set place as a result of this. To exactly synchronize the rotation of the Earth, GEO satellites should travel at a speed of around 3 km per second at an altitude of 35 786 km. This is substantially further away from the Earth's surface than many satellites. Satellites that must remain continually over one location on Earth, such as telecommunication satellites, utilize GEO. This allows an antenna on Earth to be fixed so that it is always aimed at the satellite. Weather monitoring

satellites may also utilize it since they can continuously observe particular locations to understand how weather patterns evolve there. Satellites in GEO cover a huge area of the Earth, thus as few as three satellites spread evenly can offer near global coverage. This is because a satellite at this distance from Earth can cover enormous areas at once. This is similar to being able to see more of a map from a meter distance than from a centimeter away. To observe the entire Earth from GEO, many fewer satellites are required than at a lower altitude [2].

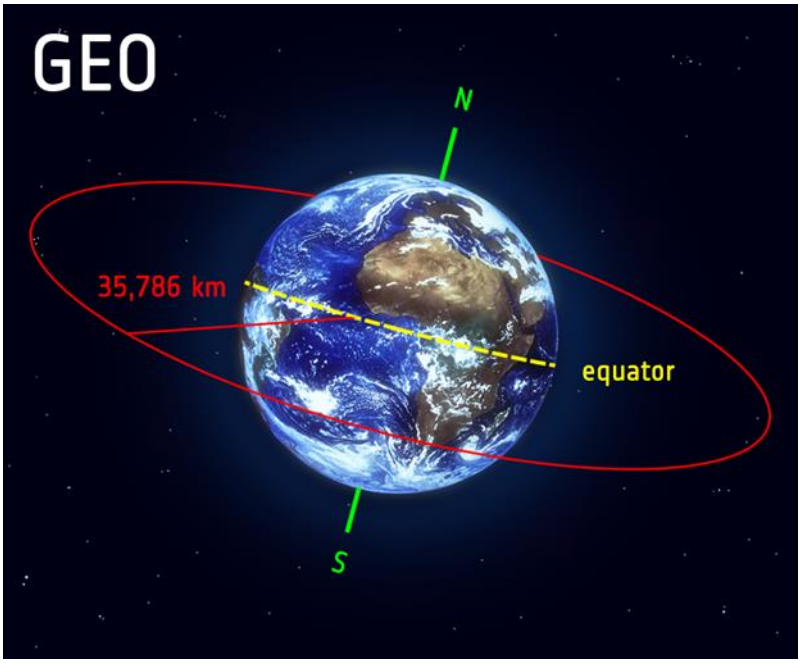

Figure 1-4 Geostationary orbit

1.2.4 importance of satellites

Satellites' bird's-eye vision allows them to see enormous portions of the Earth at once. Because of this capability, satellites can capture more data faster than ground-based devices. Satellites can also look further into space than terrestrial observatories. This is because satellites travel over clouds, dust, and molecules in the atmosphere, which can obscure views from the ground.

TV transmissions did not go very far before satellites. Television transmissions can only travel in straight lines. As a result, instead of following Earth's curvature, they would swiftly disappear into space. They were occasionally obstructed by mountains or large buildings. Phone calls to distant locations were also problematic. Installing telephone cables across large distances or underwater

is challenging and expensive. TV transmissions and phone calls are sent to satellites. The satellite may then transmit them back down to various areas on Earth relatively immediately [3].

1.2.5 Satellites sources of energy

Spacecraft have instruments that help them take pictures and collect information in space. But they need electricity to power those instruments and send the information back to Earth. To choose the best power system for a spacecraft, engineers have to think about several things. Some factors they consider are: where the spacecraft is traveling, what it plans to do there and how long it will need to work. A spacecraft generally gets its energy from at least one of three power sources: the Sun (solar energy), batteries or unstable atoms.

a) Energy from atoms

An atom is a tiny building block of matter. Atoms make up almost everything we know in the cosmos. Atoms must store a lot of energy in order to stay together. However, certain atoms, known as radioisotopes, are unstable and begin to disintegrate. As the atoms disintegrate, they release energy in the form of heat.

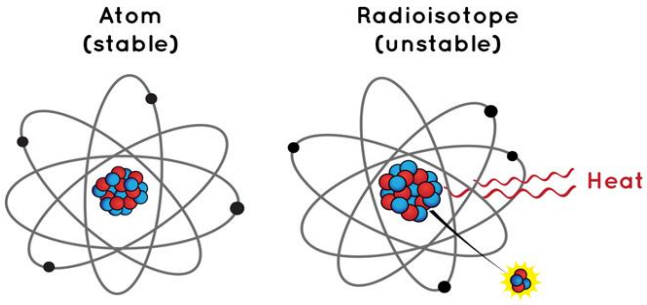

Figure 1-5 unstable atom

To generate electricity, a radioisotope power system leverages the temperature differential between the heat from unstable atoms and the cold of space. Many NASA missions have been powered by this sort of equipment. It has, for example, powered expeditions to Saturn and Pluto, as well as spacecraft that have traveled into interstellar space. This sort of power system also powers the Curiosity rover on Mars.

Radioisotope systems provide electricity for extended periods of time, even in severe conditions. This form of power is used by NASA's two Voyager spacecraft. They have flown further than any other human-made object and are still transmitting data after more than 40 years in space [4].

b) Solar energy

The sun is a 1391000 km diameter pseudo-spherical star. It is 149598000 kilometers away from land on average. Its speed is 300,000 km/s, and it takes around 8 minutes to reach land. The sun continually emits a vast quantity of radiant energy into the solar system, and the earth intercepts only a very small portion of this energy. The solar constant is equal to 1367W/m2 because an average of 1367 watts reaches every square meter from the outer edge of the Earth's atmosphere (for an average Earth-Sun distance of 150 million km)[5].

Sun energy is referred to as solar power. Satellites, which orbit Earth, are situated close enough to the Sun to frequently harness its energy. These spacecrafts contain solar panels that turn solar energy into the electricity needed to power them with a certain efficiency.

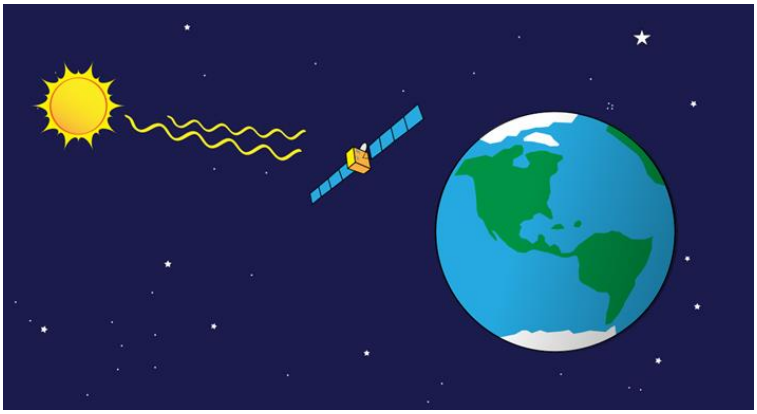

Figure 1-6 Solar Energy

Large solar panels are used on spacecraft that are orbiting far from the Sun to provide them with the energy they require. For illustration, NASA's Juno spacecraft orbits Jupiter using solar energy the entire time. The three solar arrays on Juno are each 30 feet (9 meters) long.

Figure 1-7 NASA's Juno spacecraft is powered by very large solar arrays. It began orbiting Jupiter in 2016

However, solar power is not suitable for every spacecraft. One explanation is that solar power gets less effective as spacecraft move further away from the Sun. Solar-powered explorers may also be limited by the weather and seasons of a planet, as well as severe radiation (a type of energy). They may also be unable to traverse dark, dusty areas like tunnels on the Moon. When solar power fails, spaceships must rely on other sources of electricity. As a result, scientists devised alternate power sources for these spacecrafts. One approach is to simply utilize batteries to store energy for a spaceship to use later [4]. The energy produced is then stored in electrochemical batteries in order to power the satellite during eclipse phases or when the instantaneous consumption is greater than the generators' output, and sometimes missions are designed to last a short amount of time (space probes), so a battery provided enough power for the lander to do its job.

Spacecraft batteries are built to endure. They must work in harsh locations such as space and on the surfaces of other worlds. The batteries must also be recharged numerous times. NASA scientists have developed methods to upgrade these batteries over time. They can now store more energy in smaller sizes and last longer [4].

1.3 PV cells

1.3.1 History

The physical phenomenon responsible for converting light to electricity-the photovoltaic effect-was first observed in 1839 by a French physicist, Edmund Becquerel. Becquerel noted a voltage appeared when one of two identical electrodes in a weak conducting solution was illuminated. The PV effect was first studied in solids, such as selenium, in the 1870s.

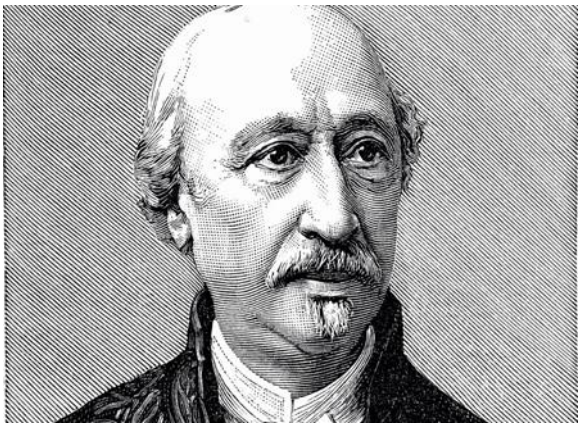

Figure 1-8 Alexander Edmund Becquerel (1820-1891)

In the 1880s, selenium photovoltaic cells were built that exhibited 1%-2% efficiency in converting light to electricity. Selenium converts light in the visible part of the sun's spectrum; for this reason, it was quickly adopted by the then-emerging field of photography for photometric (light-measuring) devices. Even today, light-sensitive cells on cameras for adjusting shutter speed to match illumination are made of selenium.

Selenium cells have never become practical as energy converters because their cost is too high relative to the tiny amount of power they produce (at 1% efficiency). Meanwhile, work on the physics of PV phenomena has expanded.

In the 1920s and 1930s, quantum mechanics laid the theoretical foundation for our present understanding of PV. A major step forward in solar-cell technology came in the 1940s and early 1950s when a method (called the Czochralski method) was developed for producing highly pure crystalline silicon.

In 1954, work at Bell Telephone Laboratories resulted in a silicon photovoltaic cell with a 4% efficiency. Bell Labs soon bettered this to a 6% and then 11% efficiency, heralding an entirely new era of power-producing cells.

A few schemes were tried in the 1950s to use silicon PV cells commercially. Most were for cells in regions geographically isolated from electric utility lines. But an unexpected boom in PV technology came from a different quarter.

In 1958, the U.S. Vanguard space satellite used a small (less than one-watt) array of cells to power its radio. The cells worked so well that space scientists soon realized the PV could be an effective power source for many space missions. This is when A cell with a yield of 9% is developed. The first satellites powered by solar cells are sent into space.

Technology development of the solar cell has been a part of the space program ever since [6].

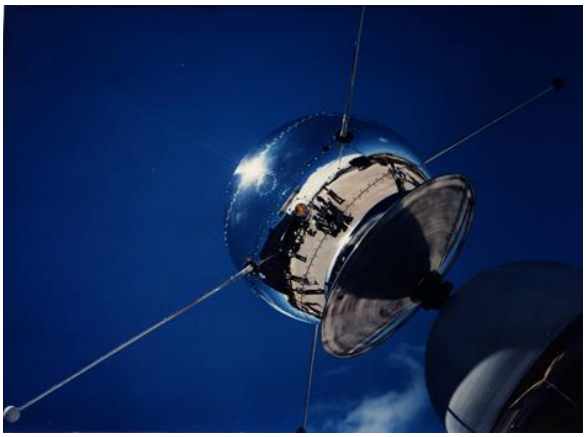

Figure 1-9 Vanguard 1-The first satellite to use solar cell power

1.3.2 Photovoltaic effect

The photovoltaic effect used in solar cells makes it possible to directly convert light energy from solar rays into electricity through generation and transportation in a semiconductor material of positive and negative electric charges under the effect of the light. This material has two parts, one with excess electrons and the other with a deficit in electrons, said respectively N-type doped and P-type doped [7].

When sunlight strikes the N-type side of a solar cell, it excites the electrons within the cell. They're so eager to get going that if directed to the P-type side of the cell, they'll gladly take it. This path includes a connection between the cell's positive and negative sides. This positive-negative junction (or PN junction) functions as a diode, allowing electrons to move from the positive (bottom) side of the cell to the negative (front) side but not the other way around. This indicates that electrons move from the negative side of the cell to the positive side of the cell via the circuit. As more electrons flow from the negative to positive sides of the cell, the electrons on the positive side are pushed up through the PN junction to the negative side of the cell, and this process continues as long as sunlight is present. The PN junction keeps electrons moving through the circuit. Figure 1-10 displays a solar cell and a PN junction [8].

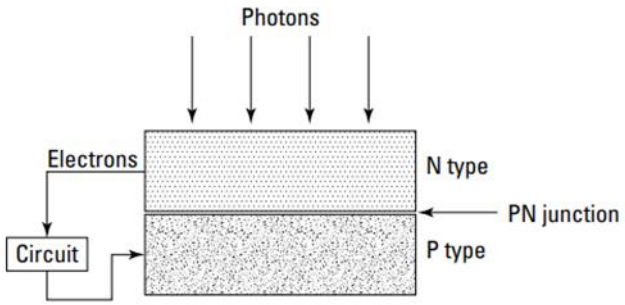

Figure 1-10 A solar cell with a PN junction.

1.3.3 Types of PV cells

PV technologies are classified as first, second, and third generation. First generation technology is the basic crystalline silicon (c-Si). Second generation includes Thin Film technologies, third generation includes concentrator photovoltaics, organics, and other technologies [9].

1. **First generation (Crystalline silicon technology)**

   Crystalline silicon cells are made from thin slices (wafers) cut from a single crystal or block of silicon. The type of crystalline cells depends on how the wafers are produced. The main types of crystalline cells are:

   1 - Mono crystalline (mc-Si)

   2 - Polycrystalline or multi crystalline (pc-Si)

   3 - Ribbon and sheet-defined film growth (ribbon/sheet c-Si)

   Crystalline silicon PV cells are the most commonly used solar cells in commercially available solar panels, representing more than 85% of global PV cell sales in 2011. Crystalline silicon PV cells exhibit energy conversion efficiency in the laboratory of more than 25% for single-crystal cells and more than 20% for multi-crystalline cells. Under standard test conditions, however, industrially made solar modules currently reach efficiencies ranging from 18% to 22% [9].

2. **Second generation (Thin films)**

   Thin film modules are made by depositing extremely thin layers of photosensitive material on low-cost supporting materials like glass, stainless steel, or plastic. Following the attachment of the deposited material to the backing, it is laser-cut into many thin cells. Thin film modules are typically frameless and encased between two layers of glass. The module is flexible if the photosensitive material is placed on a thin plastic film. This opens up the possibility of incorporating solar power generation into the fabric of a building (BIPV) or end-user application. Commercially accessible thin film kinds include :

   A. **Amorphous silicon (a-Si)**

      Amorphous silicon can absorb more sunlight than c-Si structures. A lower flow of electrons is generated which leads to efficiencies that are currently in the range of 4 to 8%. [9]

   B. **Multi-junction Thin Film silicon (a-Si/µc-Si)**

      Multi-junction silicon consists of an a-Si cell with additional layers of a-Si and micro-crystalline silicon (µc-Si) applied to the substrate. The µc-Si layer absorbs more light from the red and near-infrared part of the light spectrum. The increases efficiency by up to 10%

C. Cadmium telluride (CdTe)

CdTe Thin Films cost less to manufacture and have a module efficiency of up to 11%. This makes it the most economical Thin Film technology currently available.

D. Copper, indium, gallium, (di) selenide / (di) sulphide (CIGS) and Copper, indium, (di) selenide /(di) sulphide (CIS)

This Thin Film technology offer the highest efficiencies of all Thin Film technologies. Efficiencies of 20% have been achieved in the laboratory, which are close to the levels achieved with c-Si cells.

3. Third generation

A. Multijunction III-V Photovoltaics

High-efficiency multijunction devices use multiple bandgaps, or junctions, that are tuned to absorb a specific region of the solar spectrum to create solar cells having record efficiencies over 45%. The maximum theoretical efficiency that a single-bandgap solar cell can achieve with non-concentrated sunlight is about 33.5%, primarily because of the broad distribution of solar emitted photons. This limiting efficiency, known as the Shockley-Queisser limit, arises from the fact that the open-circuit voltage (Voc) of a solar cell is limited by the bandgap of the absorbing material and that photons with energies below the bandgap are not absorbed. Photons that have energies greater than the bandgap are absorbed, but the energy greater than the bandgap is lost as heat.

Multijunction devices use a high-bandgap top cell to absorb high-energy photons while allowing the lower-energy photons to pass through. A material with a slightly lower bandgap is then placed below the high-bandgap junction to absorb photons with slightly less energy (longer wavelengths). Typical multijunction cells use two or more absorbing junctions, and the theoretical maximum efficiency increases with the number of junctions.

In the past, multijunction devices have primarily been used in space, where there is a premium placed on lightweight power generation, which allows for the use of this relatively high-cost solar technology. For terrestrial applications, the high costs of these semiconductor substrates (compared to silicon, for example) may be offset by using concentrating optics, with current systems primarily using Fresnel lenses [10].

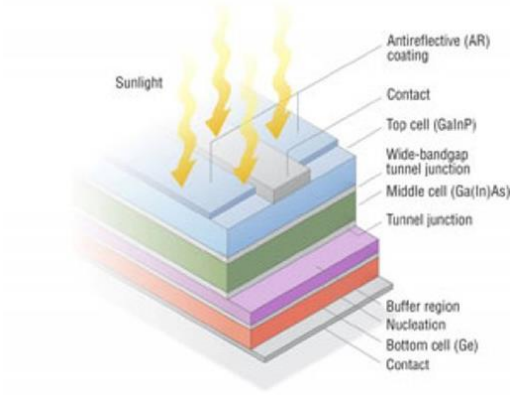

Figure 1-11 Multijunction III-V Photovoltaics structure

B. Concentrator photovoltaics (CPV)

Concentrator photovoltaics utilize lenses to focus sunlight on to solar cells. The cells are made from very small amounts of highly efficient, but expensive, semiconductor PV material. CPV cells can be based on silicon or III-V compounds (generally gallium arsenide or GaA). CPV systems use only direct irradiation. They are most efficient in very sunny areas which have high amounts of direct irradiation. The modules have precise and accurate sets of lenses which need to be permanently oriented towards the sun. This is achieved through the use of a double-axis tracking system [9].

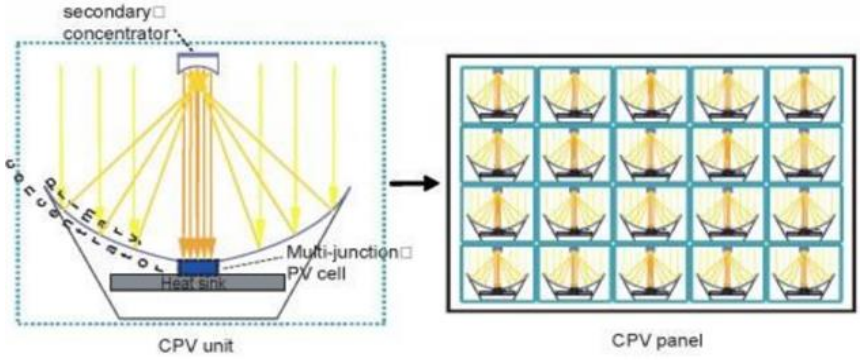

Figure 1-12 CPV unit and panel

C. Organic photovoltaics (OPV)

Organic photovoltaic (OPV) solar cells aim to provide an Earth-abundant and low-energy production photovoltaic (PV) solution. This technology also has the theoretical potential to provide electricity at a lower cost than first- and second-generation solar technologies. Because various absorbers can be used to create colored or transparent OPV devices, this technology is particularly appealing to the building-integrated PV market.

Organic photovoltaics have achieved efficiencies near 11%, but efficiency limitations as well as long-term reliability remain significant barriers.

Unlike most inorganic solar cells, OPV cells use molecular or polymeric absorbers, which results in a localized exciton. The absorber is used in conjunction with an electron acceptor, such as a fullerene, which has molecular orbital energy states that facilitate electron transfer. Upon absorbing a photon, the resulting exciton migrates to the interface between the absorber material and the electron acceptor material. At the interface, the energetic mismatch of the molecular orbitals provides sufficient driving force to split the exciton and create free charge carriers (an electron and a hole) [11].

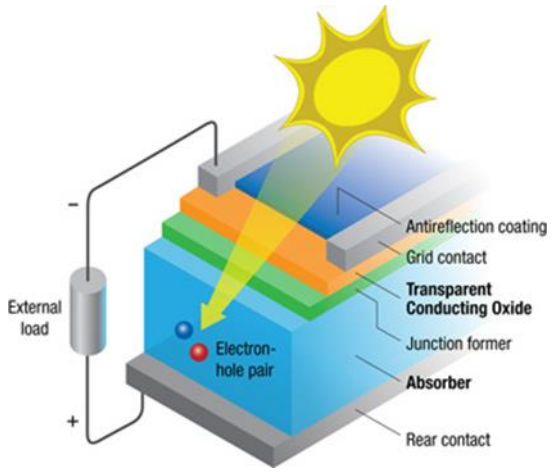

Figure 1-13 Typical structure of an organic solar cell

1.3.4 Characteristics of PV cells

1. Current-Power / Voltage Characteristics

Here is an example of a current–voltage characteristic (blue) and of the corresponding power–voltage characteristic (purple) of a solar cell under illumination. The short-circuit current density, the open-circuit voltage, the maximum power point and the voltage and current density at the maximum power point are denoted by ISC, VOC, Mpp, Vmp and Imp, respectively

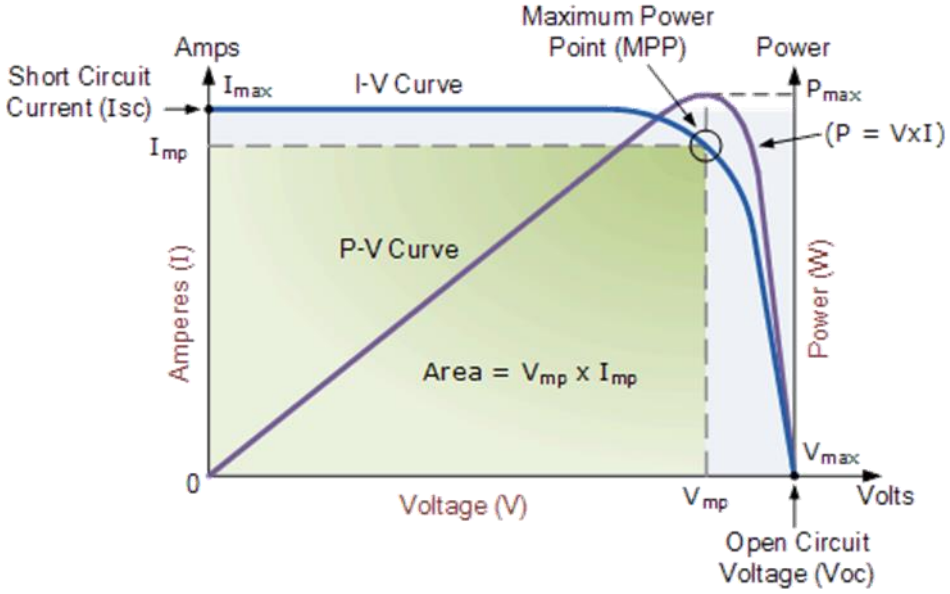

Figure 1-14 Current-Power / Voltage Characteristics

With the solar cell open-circuited, that is not connected to any load, the current will be at its minimum (zero) and the voltage across the cell is at its maximum, known as the solar cells open circuit voltage, or Voc.

At the other extreme, when the solar cell is short circuited, that is the positive and negative leads connected together, the voltage across the cell is at its minimum (zero) but the current flowing out of the cell reaches its maximum, known as the solar cells short circuit current, or Isc [12].

2. Current specifications

A. Short circuit current

Short circuit current, abbreviated Isc, is the value obtained if the positive and negative wires of a PV module come into direct contact with each other and there is essentially no resistance between the positive and negative sides of the module.

This condition is defined as voltage equaling zero since there is no potential between the two sides of the cell; the electrons are simply doing what comes naturally to them, which is to go to the electron holes. The Isc values published by manufacturers are all obtained under standard test conditions (STC)[8].

B. Maximum power current

Maximum power current (Imp) is similar to maximum power voltage Vmp in that it shows the current value when the module produces the most power feasible. The manufacturer's value is at the STC and is variable off of that. The current value varies dramatically depending on the amount of sunlight that strikes the module. When you need assistance optimizing the system's performance, use the Imp value. It should be noted that this current value is frequently utilized in conjunction with Vmp to size the system's conductors in order to maximize the power output from the modules and array [8].

3. Voltage specifications

A. Open circuit voltage

Open circuit voltage, abbreviated Voc, is the voltage value in the absence of current flow. Because the circuit is open, the resistance between the PV module's positive and negative wires is infinite. The Voc value on a PV module is at STC and changes depending on environmental conditions. When estimating the number of modules to utilize in conjunction with certain equipment, the maximum circuit voltage must be determined using the Voc value [8] .

B. Maximum power voltage

The maximum power voltage (Vmp) is, unsurprisingly, the value at which the PV module produces the greatest amount of power. This number, like the Voc, changes in reaction to the temperature of the cells. Vmp is frequently referred to as the module's operational voltage, while the true operating voltage is usually lower because of voltage loss as temperature rises. The Vmp value you see is always reported at STC. The Vmp value is significant since it is related to the current flowing from the PV modules. When considering Vmp, keep two things in mind: voltage decreases as temperatures increase, and PV modules must always have enough voltage (push) to keep the current flowing [8].

These facts imply that the Vmp value must be adjusted for high temperatures to ensure that the modules are placed in such a way that they always have enough voltage present to push the current, regardless of temperature.

4. **The maximum power point (MPP)**

   There is one combination of current and voltage at which the power of the solar cell has its maximum (Imp and Vmp, respectively). This point on the I–V characteristic of an illuminated solar cell is known as the maximum power point (mpp) [13].

$$P_{max} = I_{mp} \times V_{mp} \tag{1.1}$$

5. **Fill factor (FF)**

   The fill factor or wire factor (FF) is a significant measure derived from the I(V) characteristic that is frequently used to qualify the quality of a cell or a PV generator.

   This coefficient shows the ratio between the maximum power delivered by the cell, indicated by Pmax, and the power formed by the rectangle Isc*Voc. The bigger the value of this factor, the greater the useable power will be. The following relation defines it [13]:

$$FF = \frac{P_{max}}{I_{SC} \times V_{oc}} \tag{1.2}$$

1.3.5 Grouping of PV cells

A solar panel or a solar array is formed when PV cells are joined together, the number of cells used and the intended power output determine the size of the panel or array (the power output of a solar panel is directly proportional to the number of cells utilized). In addition to series-parallel connections, there are two main ways to connect PV cells in a solar panel or array: in series or parallel. Each connection method has advantages and disadvantages, and the choice of connection method depends on the desired output voltage and current, as well as the requirements of the specific application.

1. **Series circuit**

When PV cells are linked in series, the positive terminal of one cell is connected to the negative terminal of the following cell, and so on. The panel's overall output voltage equals the sum of the voltages of each cell. This means that a solar panel connected in series can generate more voltage than a single cell. Nonetheless, the panel's current output remains the same as that of a single cell.

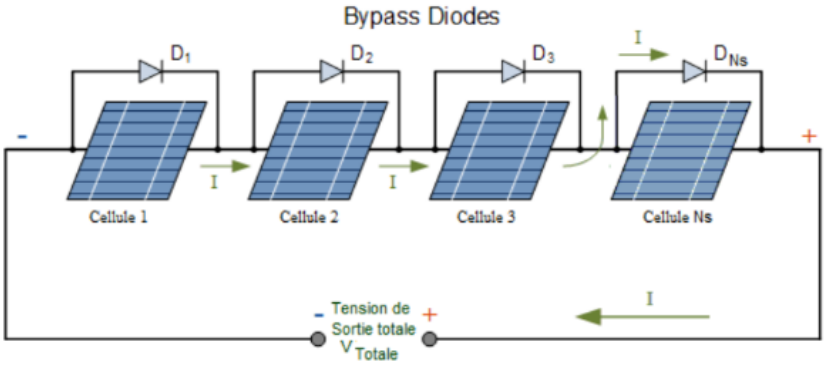

Figure 1-15 Series Connected PV Panels

2. **Parallel circuit**

When PV cells are connected in parallel, the positive terminals of all the cells are connected together, as are the negative terminals. The panel's total output current equals the sum of the currents in each cell. This indicates that a solar panel connected in parallel can generate more current than a single cell. The voltage output of the panel, however, remains the same as that of a single cell.

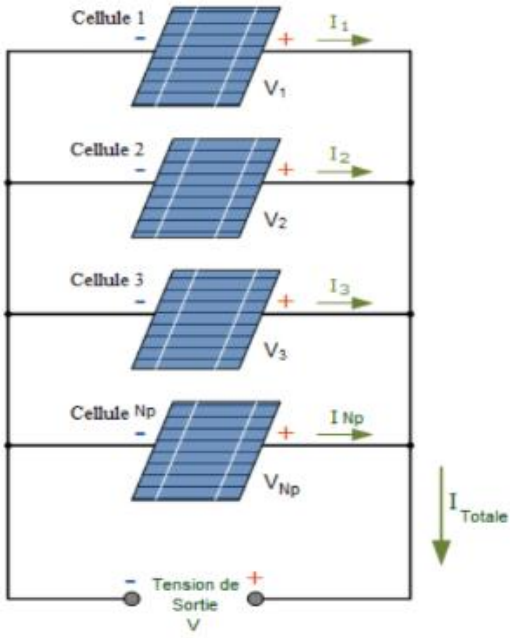

Figure 1-16 Parallel Connected Solar Panels

1.3.6 The effect of temperature on the PV cells

The temperature has a considerable impact on PV cell performance. In general, the efficiency of a solar cell decreases with increasing temperature. Because of the nature of the semiconductor materials used in PV cells, this is the case. The voltage of a module drops as the temperature of the cell rises. This is a fairly measurable and linear effect. Figure 1-17 shows how the IV curve of a typical PV module varies with temperature. Take note of how the curve travels to the left and right along the horizontal voltage axis but very little along the vertical current axis.

This movement in the curve causes the MPP to move along with the voltage, revealing that temperature variations immediately affect the voltage output, which in turn directly affects the power output.

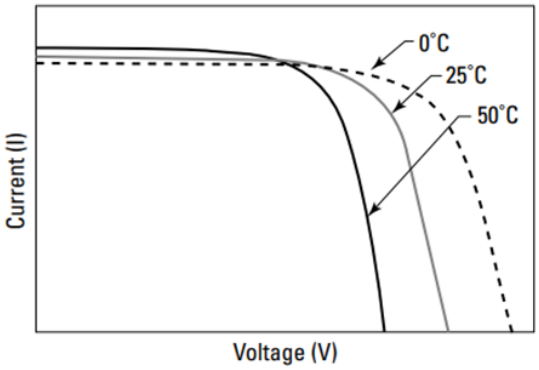

Figure 1-17 IV curves of the same module at varying temperatures

When the temperature of the PV cell rises, so does the energy of the electrons in the semiconductor's valence band. This increases the amount of electrons that may bridge the bandgap into the conduction band, hence increasing the cell's current output. However, as the temperature continues to increase, the mobility of the electrons and holes in the semiconductor material decreases, the voltage output of the cell is reduced as a result [8].

1.3.7 The effect of irradiance on the PV cells

Irradiance changes significantly throughout the day, beginning at 0 W/m2 just before daybreak and peaking at more than 1,000 W/m2 at any particular time. The quantity of irradiance that strikes a PV module directly influences how much current it can produce. This, like the voltage-temperature relationship, is a linear relationship that can be calculated over a wide variety of conditions.

Figure 1-18 illustrates how the IV curve changes with irradiance. Take note of how the curves move significantly faster vertically than horizontally. This movement illustrates that variations in irradiance have little effect on the module's voltage, despite the fact that the current is greatly altered. The MPP also moves a lot when the irradiance varies [8].

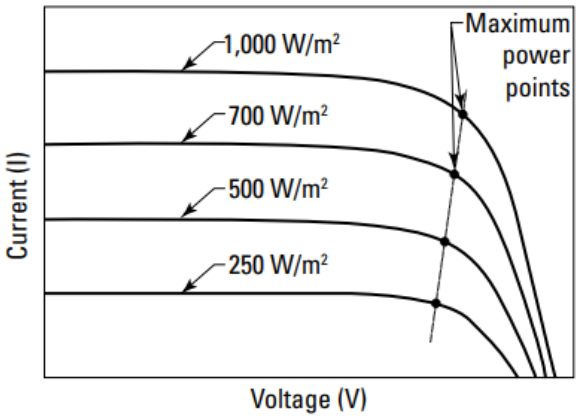

Figure 1-18 IV curves of the same module at varying levels of irradiance

Higher MPPs occur from higher irradiance levels, implying that the solar cell or PV system will produce more power. In contrast, the relationship between irradiance and MPP is not always linear and can vary depending on factors such as temperature, shadowing, and the electrical properties of the solar cell or PV system.

1.4 Conclusion

In conclusion, this first chapter provided a comprehensive overview of generalities on aerospace photovoltaic (PV) systems. The chapter began by highlighting the role of satellites and the importance of solar cells as an irreplaceable component in generating energie from the sunlight . The chapter also provide informations about solar cells with their various types and efficiencies , alongside its working principle and their electrical characteristics and we finished the chapter by discussing the effect of temperature and irradiance on PV cells. Overall, this chapter served as a foundation for understanding the generalities and key concepts related to aerospace PV systems.

CHAPTER 2.

STATE OF ART

2.1 Introduction

Devices known as solar cells can convert sunlight into electrical energy making them a popular means for environmentally friendly power production. The primary technology utilized in these devices is the single junction solar cell- formed from one semiconductor layer that absorbs light to generate electricity. Scientists have created other options such as dual junction and triple junction solar cells capable of greater efficiencies than their simpler counterpart. These innovations use many semiconductor materials arranged in varying layers capable of capturing photons over different parts of the spectrum. The dual type contains two layers while triples have three , each able to absorb wavelengths beyond what the commonplace type can due to differing energy gaps engineered into their structures. As such triple layered solar panels can capture more sun rays into electricity output produced by fewer units providing a potential shortcut towards power expenditure savings particularly valuable when resources are limited or high demand exists like at space research establishments.

To maximize benefits while mitigating risks an in depth understanding of the appealing and distracting points of each technology sort including their applications, costs, and environmental aspects is paramount.

2.2 Single Junction Solar cells

Single junction solar cells remain one of the most widely used types among all kinds of solar powered devices globally. They consist merely of a single layered semiconductor that converts light into electricity. However, despite their simplicity these devices have undergone significant technological advancements resulting in high efficiency coupled with lower production costs alike over time. Because they can supply power across different scales ranging from small consumer gadgets to big enterprises sustainable infrastructure needs single junction photovoltaics has become a necessary feature inside contemporary alternative energized context worldwide.

As a result, understanding the fundamental concepts underlying the operation of single-junction solar cells, as well as the most current advancements in their design and performance, is crucial.

2.2.1 Silicon solar cells

Although the history of silicon solar cells dates back over 50 years to the very beginning of the silicon bipolar device era, the last decade has seen enormous improvements in both the performance of experimental cells and cell theory.

Over the last few years, cells have reached performance levels once thought not to be physically attainable. As shown in figure 2-1, present laboratory cells convert over 23% of the incident energy in sunlight into electricity, well above the value of 20% once thought to be a basic limit. Silicon solar cells have different design and material requirements from most other silicon electronic devices. Not only is nearly ideal passivation of silicon surfaces required, but the bulk properties must also be of uniformly high quality for high energy conversion efficiency. This is because some wavelengths of light have to pass several hundred micrometers through the silicon before absorption and produce carriers that are still collected by the cell [14].

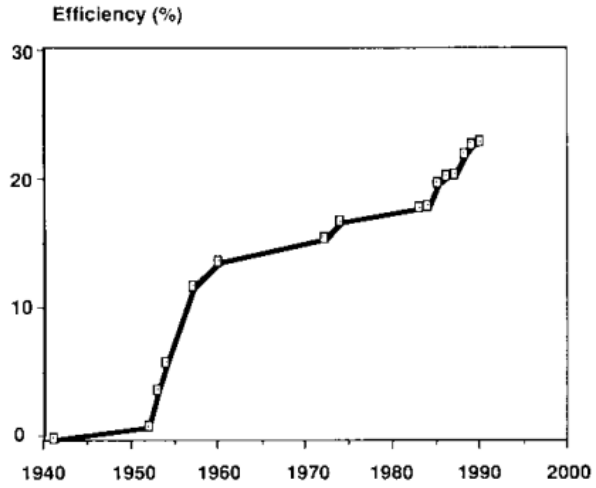

Figure 2-1 Evolution of the energy conversion efficiency of laboratory silicon solar cells

2.2.2 Crystalline Silicon Solar cells [15]

Because of its excellent efficiency, long-term stability, durability, and low cost, crystalline silicon has been intensively researched. According to studies, the efficiency of commercial wafer-based silicon modules rose from 12 % to 17 % during the previous ten years, with a decrease in average module price and a rise in cumulative photovoltaic (PV) installation up to 2018.

Some revolutionary technologies, like as screen printing, PERC, and surface texturing, played an important role in enhancing the efficiency of PV modules and lowering costs in the industries.

Since its inception, c-Si has been regarded as the sole long-term, sustainable, and high-efficiency material for solar cells. The highest performing modules in the experiment had an efficiency of 24.4 %.

A solar cell requires an innovative cell structure, optimum light absorption, a large number of effective carriers with low carrier recombination loss, minimized electrode resistance, and area reduction to attain high efficiency. Aside from the typical back surface field solar cell, several new technologies have resulted in the manufacture of a variety of high-efficiency crystalline solar cell architectures such as PERC, PERT, PERL IBC, HIT, and HBC. PERC and PERT solar cells, for example, have excellent efficiency and are also cost effective. According to studies, PERC technology accounted for 20% of the PV industry in 2017. IBC and HIT structures, for example, have very high efficiency, however the technology to produce these structures is quite costly and involves a highly complicated procedure. So let's talk about some of these high-efficiency solar cells.

A. PERC (Passivated Emitter and Rear Cell)

The PERC (Passivated Emitter and Rear Cell) structure enhances the rear surface's capacity to capture light. It was initially created at the University of New South Wales in 1983, and its design was published in a technical paper in 1989 with a then-world-record efficiency of 22.8%. The PERC technology is easier to build and less expensive.

On the back side of the conventional back surface field cell design is a metallic aluminum layer. Adding a dielectric passivation layer to the back of the PERC structure helps minimize optical and electrical losses. Al2O3/SiNx is naturally applied as the rear passivation layer. Al2O3 has an exceptional passivation. Al2O3 layer followed by SiNx layer deposition can enhance the passivation effect. The SiNx layer prevents metallization of the back passivation film. Due to the thinness of the Al2O3 layer, the SiNx layer compensates for the thickness of the rear passivation stack and produces an internal reflection on the back of the cell. Consequently, the long-wave responsiveness and short-circuit current are boosted. Laser contact opening is widely used to remove the dielectric passivation layer locally, hence facilitating the creation of Al-silicon contacts. Figure 2-2 depicts the fundamental construction of a PERC solar cell.

In 2016, the German firm Solar World achieved a PERC solar cell efficiency of 21.7%. Trina Solar in China established an efficiency record of 22.13 % later that year. On a big substrate (156 mm X 156 mm), the polycrystalline PERC solar cell achieved an efficiency of 21.25 %,

but Jinko Solar immediately beat the record with an efficiency of 21.63 %. Jinko Solar achieved a record efficiency of 22.04 % for a polycrystalline solar cell in 2017, breaking the previous mark of 22.0%. LONGI Solar has achieved a PERC structural efficiency record of 24.02 %, according to their most recent data (2019).

Enhanced emitter topologies, wafers with longer lives, multiwire in place of busbars, and so on, should be among the important developments in PERC solar cells. According to the International Photovoltaic Technology Roadmap, the worldwide market share of PERC technology topped 20 % in 2017 and is anticipated to approach 60 % during the next decades.

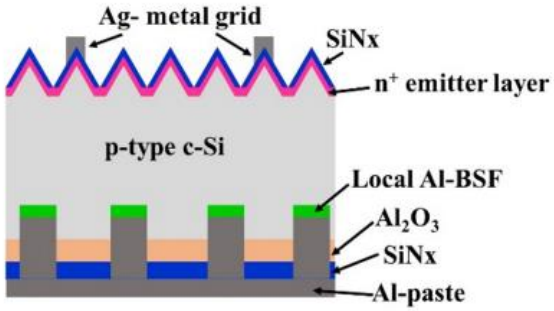

Figure 2-2 PERC solar cell structure

PERL and PERT cells are two more structures in the PERx family that have attracted interest owing to their potential to reduce recombination loss while achieving high VOC and efficiency. These structures may be created by depositing a poor recombination and insulating layer on the back side of the absorber, followed by a local ablation to provide metal contacts to the absorber. Despite the fact that PERT and PERL structures are frequently used, they require an industrially practical production method. Future PERL and PERT cell research should concentrate on the development of emitter layer doping and local BSF processes to ensure damage-free high-quality production of doped areas.

B. IBC Solar cells (Interdigitated Back Contact)

One of the most significant forms of crystalline solar cells is the IBC (Interdigitated Back Contact) solar cell. One of its benefits is that it may aid in the development of a tailored idea that meets the energy needs of localized situations.

IBC cells use the following innovation: the contacts are situated on the cell's back side rather than the front. Because of the reduced shadowing on the front of the cell, it can achieve a better

efficiency, at the same time, electron-hole pairs formed by the absorbed light may still be collected on the back side of the cell. In the 1980s, Stanford University produced the first IBC solar cell, which attained a 21.3 % efficiency.

For optimal light trapping on silicon wafers, the IBC solar cell production method includes front surface texturing with random pyramids. The back surface has been polished. POCl3 diffusion or ion implementation is used to create the front and rear surface fields. Screen printing or lithography is used to define the rear emitter pattern. The emitter and back-surface field doping layers are both situated on the cell's rear side in an interdigitated arrangement. Figure 2-3 is a schematic design of an IBC solar cell.

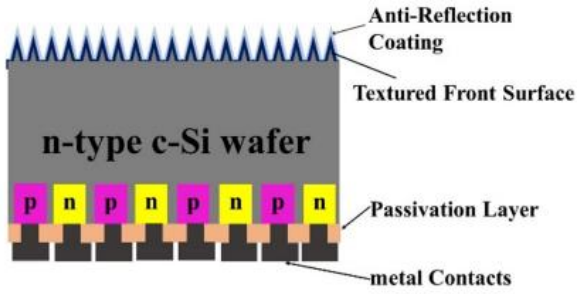

Figure 2-3 IBC solar cell structure

The use of all of the cell structure's rear connections minimizes optical shading losses on the front side. As a result, the IBC solar cell's short-circuit current density and absorption capacity rise.

Other benefits include:

1) the absence of front metal fingers, which allows for greater room.
2) reduced series resistance on the back side.
3) simpler module designs.

IBC solar cells are mainly made on n-type silicon substrates with boron-diffused emitters. A pyramid structure with an anti-reflective coating layer is used to increase the light trapping effect. The thermal SiO2 passivation layers on the front and back surfaces exhibit a long-wave response and decreased surface recombination. A metal electrode is produced, allowing for point contact with the silicon substrate. By removing the front grids and busbars, the effective area of the absorption may be enhanced. An increase in effective area leads to an increase in photo-absorption capacity. However, this cell design still has to be improved.

Several issues develop during the operation of multiple lithography. The expenses of avoiding non-uniform distribution and high-temperature damage rise. A boron-doped diffusion mask layer and an interdigitated structure printed on the back surface can simplify the procedure. Protections against non-uniform distribution and high-temperature damage, on the other hand, greatly raise the cost. Furthermore, the screen-printing technique is inaccurate in terms of alignment and printing reproducibility.

To circumvent these issues, doping by ion implementation is widely used since it allows for fine control of the doping concentration and the development of uniform p- and n-regions with adjustable junction depth. This doping process necessitates a high annealing temperature, which is difficult to obtain in the PV sector. Laser doping techniques are utilized as an alternative. It provides consistent doping concentration and depth controllability, as well as pattern ability in the doping area. The selective doping region shields the entire silicon from high temperature damage. Other advantages of laser doping include laser texturing, laser ablation for contact opening, and laser-fired contacts in solar cells.

In the original edition, IBC solar cells had an efficiency of 21.3 %. SunPower attained a record efficiency of more than 24% in 2010. SunPower achieved the maximum efficiency of 25.2 % for IBC structure in 2016.

IBC cells are highly appreciated in applications requiring greater current values, such as CPV, solar race cars, and even solar aircrafts. According to the International Technology Roadmap study from 2018, IBC cells have an 8% share of the worldwide market, which is predicted to expand by at least 5% over the next ten years.

C. HIT Solar cells

The intrinsic thin layer, which is the core of the HIT solar cell, is comprised of the silicon heterojunction. A HIT solar cell is made up of a tiny monocrystalline silicon wafer surrounded by ultra-thin amorphous silicon layers. Sanyo Co. Ltd (now Panasonic Co. Ltd) created and named this cell in 1991. The benefit of this cell is that it can successfully distinguish electron hole pairs. The hydrogenated amorphous silicon (a-Si(H)) layer has an excellent passivation effect on the crystalline silicon surface. It reduces surface recombination by lowering the interface state density. These two characteristics enable the HIT solar cell to have a high open circuit voltage and a high efficiency.

Other advantages of the HIT cell include:

1- It features structural symmetry, which minimizes cell thickness and production cost. The bifacial module made up of these symmetrical HIT cells can absorb light from both sides. As a result, the generating capacity can be enhanced.

2- This solar cell design may be manufactured at low temperatures (below 200°C).

3- There is significant band bending between amorphous Si and crystalline Si.

4- The crystalline Si surface has good surface passivation.

5- It is stable.

Figure 2-4 is a schematic of the HIT solar cell. On the front side, an inherent amorphous Si layer and a p-type amorphous silicon layer are formed to produce a p-n region. The back-surface field consists of stacked symmetrical layers of intrinsic amorphous Si and n-type amorphous Si. By screen printing and sputtering, respectively, a metal electrode and a TCO layer are subsequently fabricated.

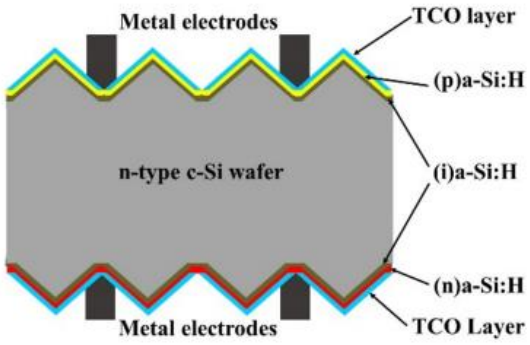

Figure 2-4 HIT solar cell structure

The entire procedure is carried out at temperatures below 200 degrees Celsius. Since then, scientists have concentrated on the following aspects:

1-decrease in optical and electrical loss.

2-cleaning of the c-Si wafer.

3-development of high-quality wide-gap alloys and high carrier mobility.

4-reduction in the cost of wafers with a smaller thickness.

In 2013, their efforts yielded an efficiency of 24.7% (VOC = 750 mV, JSC = 39.5 mA/cm2, FF = 83.2%). Kaneka reported the best efficiency for an HIT solar cell in 2015, at 25.1% (VOC = 738 mV, JSC = 40.8 mA/cm2, FF = 83.5%). Using a tunneling oxide passivation layer, Silevo Inc. manufactured a large-area (239 cm2) solar cell panel. It attained a 23.1 % conversion

efficiency (VOC = 739 mV, JSC = 39.9 mA/cm2, FF = 80.5 %). The CESM in Switzerland and Meyer Burger obtained a greater conversion efficiency in the range of 22,4% 22,7%. The Shanghai Institute of Microsystem and Information Technology has attained an efficiency rate of 23,1 % and has pushed for further industrialization on a broad scale. According to the International Technology Roadmap for Photovoltaics, the HIT solar cell has a technical potential for cost reduction, and its worldwide market share might expand by as much as 10 % in the next years. To do this, the thickness of the Si wafer must be decreased, the TCO materials must be enhanced, and the metal electrode must be tuned.

D. HBC Solar cells

The Heterojunction Back Contact solar cell was created by applying the integrated back contact idea to the heterojunction structure. The IBC solar cell is not shielded in any way. Consequently, its short circuit current density JSC is high and its passivation quality is maintained. This causes an elevated open-circuit voltage. Figure 2-5 depicts a schematic of the HBC solar cell. A passivation layer is produced on the c-Si wafer's front surface. It has a low level of surface recombination and excellent transparency.

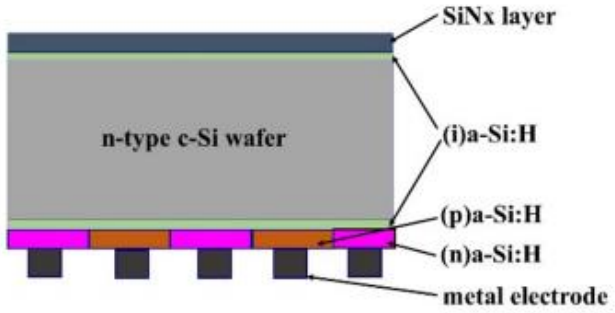

Figure 2-5 HBC solar cell structure

A coating of anti-reflective silicon nitride is then placed. Afterwards, two stacking layers are deposited on the back surface, followed by the electroplating of grid electrodes onto the p-type and n-type layers. The back grid electrodes can significantly increase the solar cell's fill factor. LG manufactured the first developed HBC solar cell in 2012, which had an efficiency of 23.4% at the time. Later, in 2014, Sharp attained a conversion efficiency of 25.1% (VOC = 736 mV, JSC = 41.7 mA/cm2, FF = 82%). Concurrently, Panasonic created a solar cell with a surface area of 143.7 cm2 and a conversion efficiency of 25.6%. In 2016, Kaneka Corporation reported

a conversion efficiency of 26.33 % (VOC = 744mV, JSC = 42.3 mA/cm2, FF = 83.8 %), but the best conversion efficiency measured for an HBC solar cell to far is 26.6 % (VOC = 740 mV, JSC = 42.5 mA/cm2, FF = 84.6 %). This 0.3 % increase is a result of the enhanced fill factor.

2.2.3 Equivalent model

A. single diode model

Figure 2-6 shows the most common equivalent circuit of a single junction solar cell based on a diode and resistance. In the case of a perfect solar cell, A current source and a diode are connected in parallel, the current source models the photon-generated current and the diode models the PN junction. In the case of a real solar cell, the equivalent circuit must include a series resistance Rs that models the photocell's resistive losses and a shunt resistance Rp that models the leakage currents that bypass the junction [16].

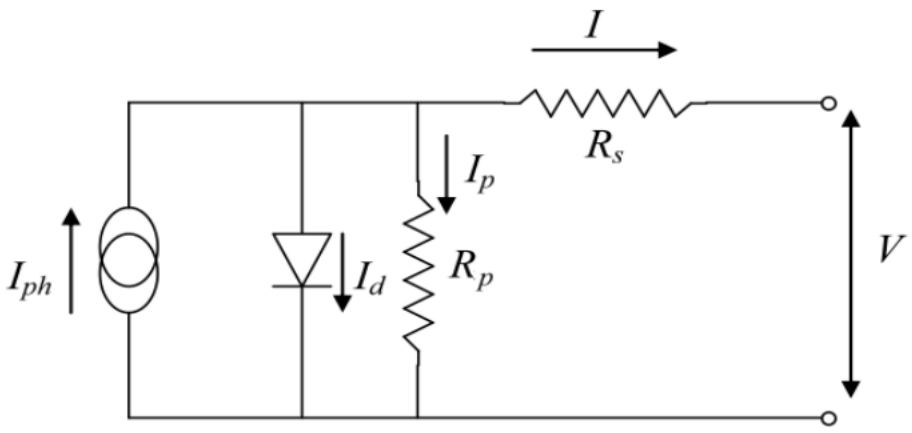

Figure 2-6 equivalent circuit of a single diode SJSC

Analyzing the equivalent circuit, total current I could be found using Kirchhoff current law

$$I = I_{ph} - I_d - I_p \tag{2.1}$$

Where: I_{ph}, I_d and I_{sh} are photon current in ampere, diode's current in ampere and parallel resistance current respectively. So, the total current equation is:

$$I = I_{ph} - I_S\left(e^{\frac{q(V+IR_S)}{nKT}} - 1\right) - \frac{V + IR_s}{R_p} \quad (2.2)$$

B. Double diode model

The well-known double-diode model displayed in Figure 2-7 is used to represent the physics of a monocrystalline silicon PV module because it describes its behavior more accurately than the single-diode model under low-irradiance conditions. Furthermore, this model is widely acknowledged as accurately representing the behavior of polycrystalline silicon PV modules. Single- and double-diode models, which were created and widely utilized in the past primarily for PV cells, have frequently been used to PV modules and arrays as well. One diode represents the diffusion current in the p-n junction, while the other is added to account for the space-charge recombination effect.

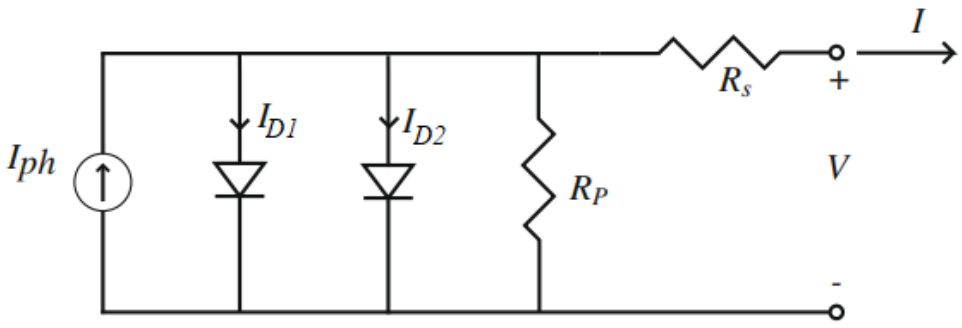

Figure 2-7 equivalent circuit of a double diode SJSC

the current is given by the equation:

$$I = I_{ph} - I_{S1}\left(e^{\frac{q(V+IR_S)}{n_1KT}} - 1\right) - I_{S1}\left(e^{\frac{q(V+IR_S)}{n_1KT}} - 1\right) - \frac{V + IR_s}{R_p} \quad (2.3)$$

Based on the basic research of single diode and double diode models, single diode should be favored for energy power system planning objectives. However, the double diode model provides more accurate and precise characteristics under changeable weather circumstances at the expense of longer iterations and harder parametric calculations [16].

2.3 Dual Junction Solar cells

Each junction in a dual junction solar cell is often built of a different semiconductor material, which is carefully chosen to optimize the absorption of different wavelengths of light. This enables the solar cell to capture a greater range of photons from the sun, including both high-energy and low-energy photons. The bandgap engineering idea behind the dual junction solar cell concept. varying semiconductor materials have varying bandgaps, which govern how much energy they can absorb from photons. Dual junction solar cells can successfully exploit a larger range of solar energy by mixing materials with distinct bandgaps, boosting their overall conversion efficiency.

2.3.1 Types of dual junction solar cells

These are only a few examples of the various varieties of dual junction solar cells available. Each design seeks to maximize the absorption of different regions of the solar spectrum, hence boosting the overall efficiency of the solar cell.

A. Amorphous silicon/crystal silicon heterojunction

This model was presented by **Fang, J et all [17]**, where they demonstrated the use of a hydrogenated amorphous silicon (a-Si:H) top cell and a crystal silicon heterojunction (HIT) bottom cell to form a double-junction solar cell with a high open circuit voltage (VOC) . Their photovoltaic technology beats all previous known pure silicon-based double-junction solar cells with a high overall VOC of 1.561 V and a short current density of over 14 mA/cm2. The newly developed a-Si:H/HIT double-junction solar cells show the potential in a variety of applications

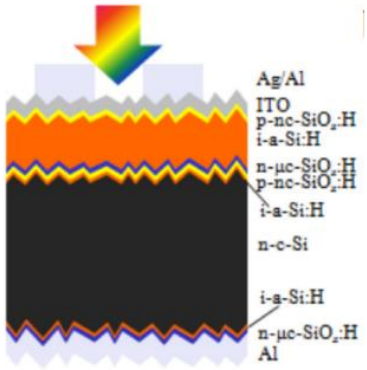

Figure 2-8 Schematic illustration of a-Si:H/HIT double junction solar cell

The a-Si:H/HIT tandem solar cell with a VOC of 1.523 V and a JSC of 14.92 mA/cm2 achieved the highest conversion efficiency of 14.26%. A maximum VOC of 1.561 V was also obtained.

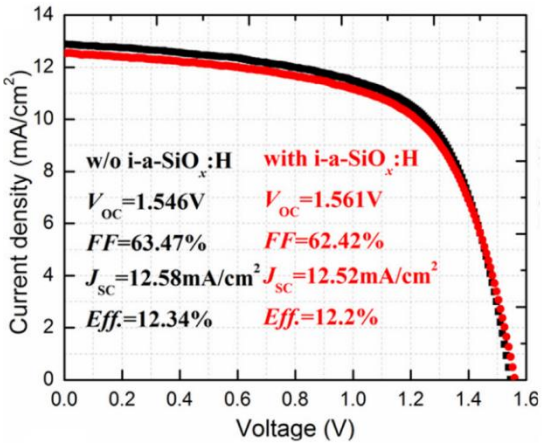

Figure 2-9 I-V characteristics comparison of the tandem solar cell with and without an i-a- SiOx:H buffer layer at i/p interface of the HIT bottom cell

By introducing an i/p interface buffer layer in the HIT bottom cell and adjusting the top cell thickness, the performance characteristics of tandem solar cells have been adjusted. An appropriate optical and electrical design was chosen to achieve high balanced light absorption and electrical output in tandem solar cells.

B. Silicon / Germanium

Alshkeili, S et all [18] presented the design of a device that can convert a wide range of the solar spectrum by utilizing a dual junction structure composed of a moderate bandgap (1.12 eV) Si cell and a narrow bandgap (0.66 eV) Ge cell, the bottom Ge solar cell expanded photon collecting to the near IR portion of the solar spectrum. The Si on Ge dual junction solar cell devices were constructed in tandem with three terminals and optimized and simulated under various temperatures and spectrum conditions using PC1D. This is a Si/Ge dual junction tandem solar cell device structure.

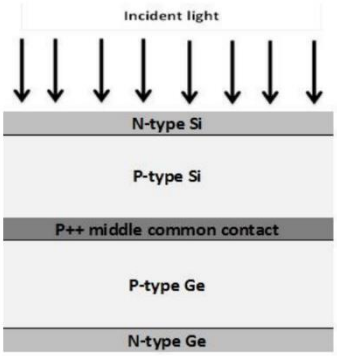

Figure 2-10 Si/Ge dual junction tandem solar cell device structure

These Si/Ge tandem devices might reach higher conversion efficiency than ordinary single junction Si cells. The usage of three terminals has shown to avoid the losses associated with tunnel junctions and current matching. These three terminals are the following:

a) Thicknesses of the top and bottom cells.

b) Depth of the junctions.

c) Doping concentrations of the active layers.

These parameters were varied independently to extract the maximum efficiency of these devices, and the optimization was performed under the standard testing conditions (STC) of AM1.5G, 25°C and 1 sun. The figure bellow represents the results:

Device total thickness (µm)	10		20		50		100	
Cell	Si	Ge	Si	Ge	Si	Ge	Si	Ge
N-type doping density ($\times 10^{18}$ cm^{-3})	5	7	5	7	7	7	5	7
P-type doping density ($\times 10^{15}$ cm^{-3})	5	1	5	1	5	1	7	10
Thickness (µm)	8	2	17.5	2.5	43	7	90	10
N-type Junction depth (µm)	0.1	0.6	0.1	0.7	0.1	0.6	0.1	0.8
Efficiency (%)	11	3.47	13.2	2.9	14.9	2.68	15.5	2.36
	14.47		16.1		17.58		17.86	
Voc (mV)	580.5	223	583.8	221.1	586.6	210.6	583.3	206.1
Isc (mA/cm^2)	23.5	22.6	28	19.3	31.4	19.1	32.8	17.3
FF	0.83	0.62	0.8	0.63	0.8	0.65	0.8	0.66

Table 1 The optimized device structures and performance of the four devices under AM1.5G, 25 °C and 1 sun

It became clear that when the Si solar cell is as thick as possible, it contributes the most to the output of the dual junction device when compared to the Ge cell. In general, increasing the entire thickness of the device enhances its efficiency, although the gain in efficiency becomes relatively minimal as shown by devices 50 m and 100 m, and the usefulness of the Ge cell in the tandem devices increases with increased concentration as it contributes about 10% to the total device efficiency under 1000 suns.

C. Gallium Indium Phosphide/Gallium Arsenide (GaInP/GaAs)

This work was done by **Ataser, T and all [19]**, a dual junction GaInP/GaAs SC structure was built utilizing an analytical solar cell model for usage in AM1.5G. InGaP/GaAs solar cells are typically fabricated using epitaxial growth techniques, in our case Molecular Beam Epitaxy (MBE) technique was used considering the optimization conditions in the design of the cell.

To investigate lattice matching between the sub-cells, the alloy composition and lattice constants of each layer in the structure were measured using High Resolution X-Ray Diffraction (HRXRD). Figures 2-11 and 2-12 show the architecture and the I-V characterization of the dual junction GaInP/GaAs.

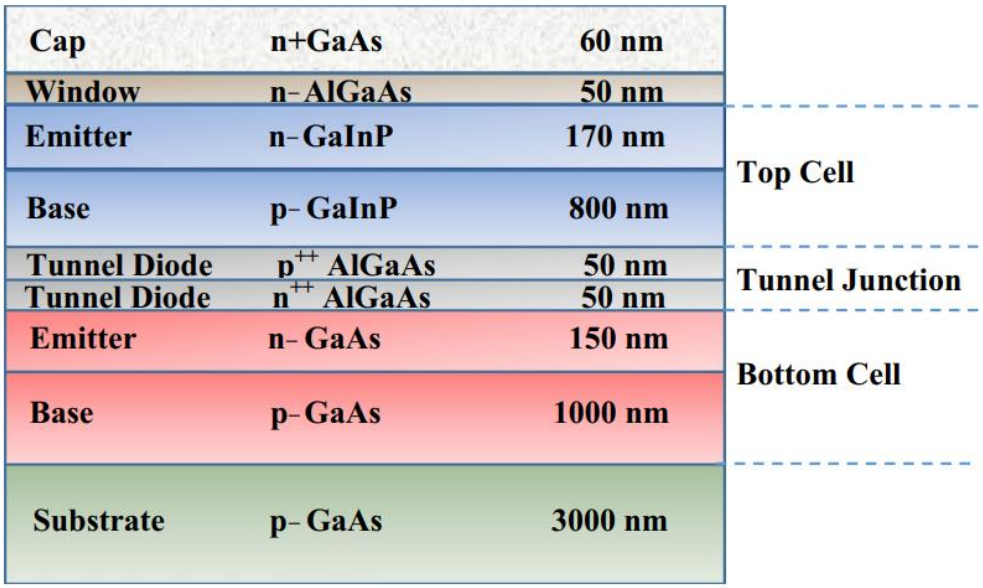

Figure 2-11 The device architecture of the dual junction GaInP/GaAs solar cell

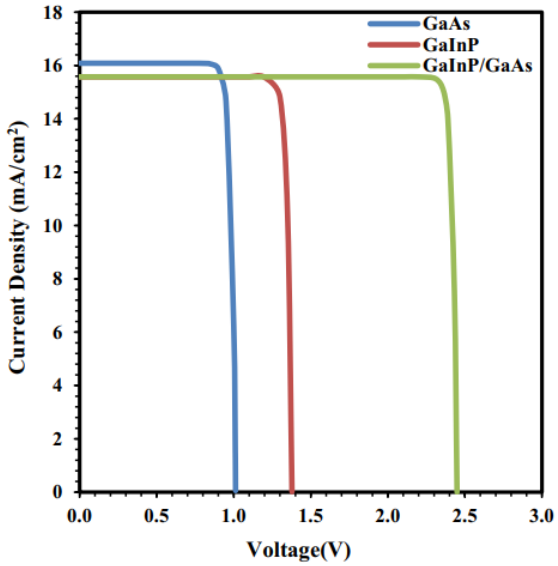

Figure 2-12 I-V characterization of the modeling dual junction GaInP/GaAs solar cell

The electrical parameters (Isc, Voc, and η) of the modeling solar cell were calculated (Isc= 15.57mA/cm² ; Voc= 2.39 v). The theoretical efficiency of DJ GaInP/GaAs SC was found to be 25.62%.

2.3.2 Equivalent model of dual junction solar cell

A. Single diode model

In this part we chose a model presented by **Yang, Terry [20]**where he mentioned dual junctions as step in his work on a triple junction solar cell, the equivalent circuit is presented in the figure below:

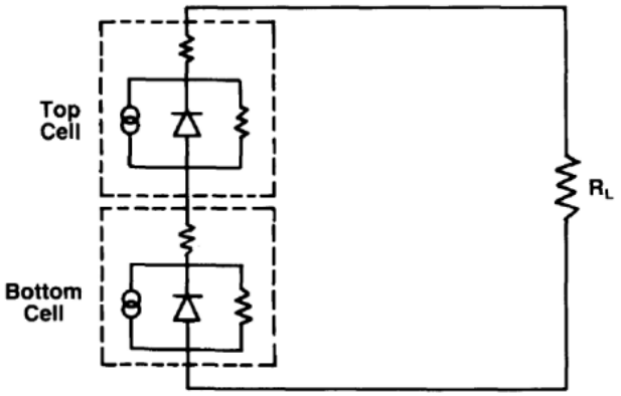

Figure 2-13 Equivalent circuit for a single diode dual junction solar cell

As mentioned earlier dual junction are composed of a top and bottom cell, and in this model the sub-cells are connected with bonding wire resistance, it serves as a conductor to carry the current generated by the solar cell and connect the different layers within the dual junction solar cell , and it may be carefully selected and optimized to minimize resistance and improve electrical performance.

B. Double diode model

Double diode model is same as mono or triple junction solar cells, figure 2-14 shows the equivalent circuit.

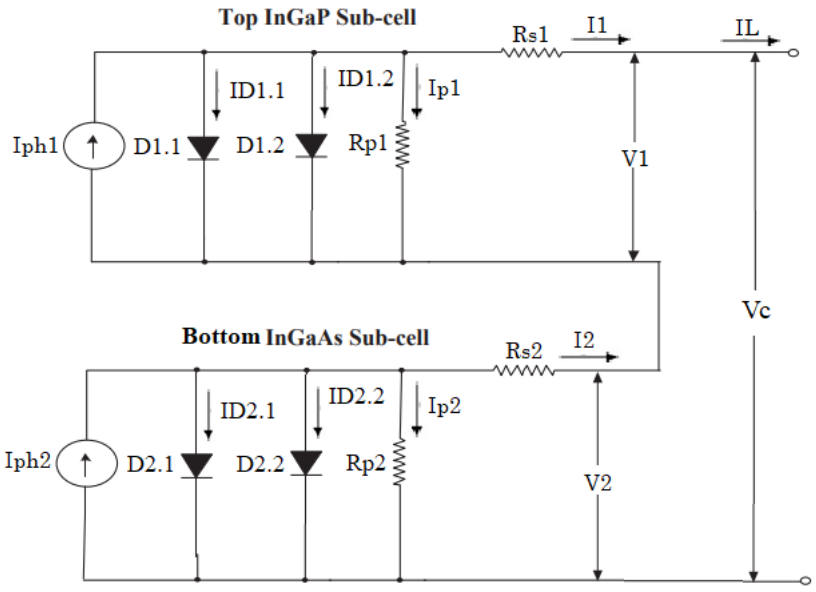

Figure 2-14 Equivalent circuit for a double diode dual junction solar cell

A double diode model in dual junction gives an illustration of the electrical properties of dual junction solar cells that is more precise and extensive, it also offers higher efficiency prediction, more flexible parameter extraction, validity over a range of diverse operating situations, as well as enhanced design optimization capabilities.

The mathematical equations going to be discussed in the triple junction part, because they have all the same principle.

2.4 Triple junction solar cells

2.4.1 Triple Junction model (Equivalent Electrical Circuit)

Triple junction InGaP/InGaAs/Ge solar cell consists of InGaP, InGaAs, and Ge subcells as shown in Fig. 2-15. The sub-cells are constructed with decreased energy gaps from the top to the bottom. This structure minimizes the losses due to thermalization of hot carriers and transmission of low energy photons that increases the solar energy converted into electricity more efficiently than single-junction cells. Multi-junction InGaP/InGaAs/Ge solar cells are known to have an ultrahigh efficiency and are now used for space applications [21].

Fig. 2-16 below demonstrates the equivalent structure of triple junction solar cells. Due to increasing requirement for power, mass and area traditional silicon solar cells will be more and more replaced by high efficiency multi-junction solar cells on space solar generators. Triple junction solar cells consist of sub cells connected in series in a way similar to the conventional one, to get high efficiency through current-matching among the generated current from each sub cells band gap energy should be strictly combined. Moreover, layers are connected together with tunnel junction and are also provided with window layers. The current generated is highly dependent on amount of light exposure. Series resistance models the tunnel resistance between each cell and the shunt resistances represent the cell material resistance. GaAs based solar cells have the potential to reach efficiencies greater than 30% [22].

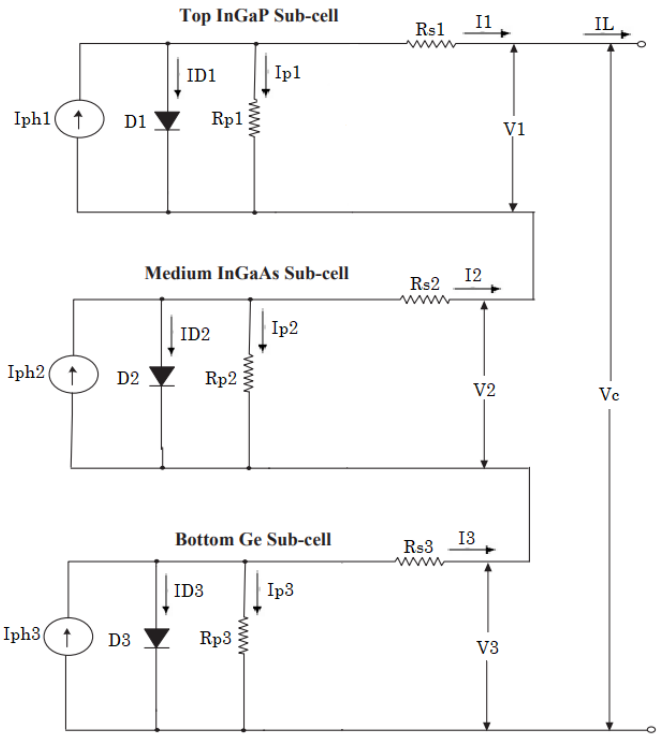

Figure 2-15 Equivalent circuit model for Triple Junction Solar cell [21]

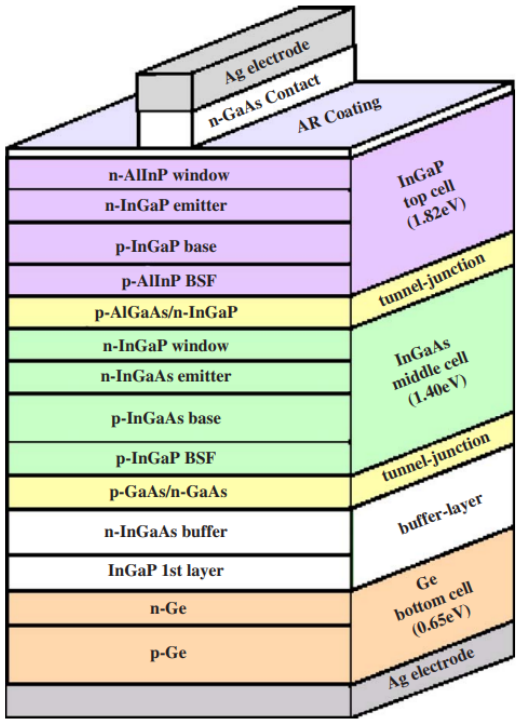

Figure 2-16 Triple junction solar cell equivalent structure

the sub cell is characterized by a current source (I_{phi}) parallelly connected to a rectifying diode Di and parallel resistance (R_{pi}) (shunt), and connected in series with a series resistance (R_{Si}). From Fig. 1 it is apparent that the current generated by each sub cell $I_{i(i=1,2,3)}$ using Kirchhoff law is given as follow [23] :

$$I_i = I_{phi} - I_{Di} - I_{pi} \tag{2.4}$$

where i equal 1 to 3 are top sub-cell, medium sub-cell and low sub cell respectively.

And I_{Di} is the diode current and I_{Pi} is the parallel resistance (shunt) current in each sub sell, they can be calculated with the followed formulas:

$$I_{Di} = I_{Si}(e^{\frac{q(V_i+I_iR_{Si})}{N_iKT}} - 1) \tag{2.5}$$

$$I_{pi} = (V_i + I_iR_{Si})/R_{pi} \tag{2.6}$$

where I_{Si} is the reverse saturation current of certain diode in A/cm2, q is the constant charge in an electron $q = 1.602 \times 10^{-19}[C]$, V_i is the cell operating output voltage, R_{Si} is the series resistance, R_{pi} is the parallel resistance, N_i is the quality factor of diode, K is Stephan Boltzmann constant $K = 1.38064852 \times 10^{-23}[m^2kg\ s^{-2}K^{-1}]$, T is the cell operating temperature [23].

By using equations (2.5) and (2.6) the equation (2.4) becomes:

$$I_i = I_{phi} - I_{Si}(e^{\frac{q(V_i+I_iR_{Si})}{N_iKT}} - 1) - (V_i + I_iR_{Si})/R_{pi} \tag{2.7}$$

as the parallel resistance R_{pi} (shunt) is higher enough than the series resistance R_{Si} , the shunt current can be neglected, the Eq. (2.7) can be simplified as:

$$I_i = I_{phi} - I_{Si}(e^{\frac{q(V_i+I_iR_{Si})}{N_iKT}} - 1) \tag{2.8}$$

The efficiency η_{PVmax} of the TJSC is the ratio of the its maximum electric generated power P_{PVmax} relative to the incident solar power P_{in}, it can be calculated as follows [23]:

$$\eta_{PVmax} = \frac{P_{PVmax}}{P_{in}} = \frac{V_{mpp} \times I_{mpp}}{P_{in}} \tag{2.9}$$

where V_{mpp} and I_{mpp} are the cell voltage and current at maximum power point, correspondently.

The temperature of the cell is considered to be uniform. The dark saturation current of a diode is very sensitive to temperature and can be found using the equation below [24]:

$$I_{Si} = k_i \times T^{\frac{3+\gamma_i}{2}} \times e^{\frac{-q \times E_{gi}}{N_i K T}} \tag{2.10}$$

Where γ_i is a constant, and E_g is the bandgap energy in eV. The band gap energy varies from cell to cell due to material differences. Because band gap energy is inversely proportional to operational temperature, its value depends on it.. The relationship between bandgap energy and temperature is described in the equation (2.11) given below [24]:

$$E_{gi} = E_g(0) - \frac{\alpha_i \times T^2}{T + \beta_i} \tag{2.11}$$

$$E_g(A_{1-x}B_x) = (1-x)E_g(A) + xE_g(B) - x(1-x)P \tag{2.12}$$

Where $E_g(0)$ is bandgap energy at 0°C, α and β are constants dependent on the materials used. The band gap energy given in equation (2.12) is strongly affected by the mixture alloys of the Indium Gallium Arsenide "InGaAs" and Indium Gallium Phosphate "InGaP". However, Germanium "Ge" is referred as pure material. The band gap for semiconductors alloys can be determined by the following linear superposition [24]

$A_{1-x}B_x$ is the alloy composition and P [eV] is an alloy dependent parameter that accounts for deviations from the linear approximation.

In equation (2.13), the voltage at the terminals of a triple junction solar cell is given by the total of the voltages of three sub-cells linked in series [25].

$$V_c = \sum_{i=1}^{3} V_i \tag{2.13}$$

The voltage can be extracted from Eq. (2.13) as follows:

$$V_c = \sum_{i=1}^{3} \frac{N_i KT}{q} \ln\left(\frac{I_{phi} - I_L}{I_{Si}} + 1\right) - I_L R_{Si} \tag{2.14}$$

Rearranging these equations, we got:

$$V_c = \frac{KT}{q}\left[n_1 \ln\left(\frac{I_{ph1} - I_L}{I_{S1}} + 1\right) + n_2 \ln\left(\frac{I_{ph2} - I_L}{I_{S2}} + 1\right) + n_3 \ln\left(\frac{I_{ph2} - I_L}{I_{S2}} + 1\right)\right] - I_L R_S \tag{2.15}$$

Where $R_S = R_{S1} + R_{S2} + R_{S3}$

Setting $I_L = 0$ leads to the open circuit voltage:

$$V_{oc} = \frac{KT}{q}\left[n_1 \ln\left(\frac{I_{ph1}}{I_{S1}} + 1\right) + n_2 \ln\left(\frac{I_{ph2}}{I_{S2}} + 1\right) + n_3 \ln\left(\frac{I_{ph2}}{I_{S2}} + 1\right)\right] - I_L R_S \tag{2.16}$$

The maximum power point (MPP) is obtained by setting $\frac{dP}{dI_L} = 0$ where the power is $P = I_L VA$.

$$I_i = I_{phi} - I_{Si.1}\left(e^{\frac{q(V_i+I_iR_{Si})}{N_iKT}} - 1\right) - I_{Si.2}\left(e^{\frac{q(V_i+I_iR_{Si})}{N_iKT}} - 1\right) \quad (2.17)$$

2.4.2 Triple Junction double diode model (Equivalent Electrical Circuit)

The model of a single diode combines the two reverse saturation current terms (recombination in the depletion and quasi neutral regions) into one term. In a broader sense, these terms are separated so that the circuit is composed of two diodes, as represented in Fig. 2-17

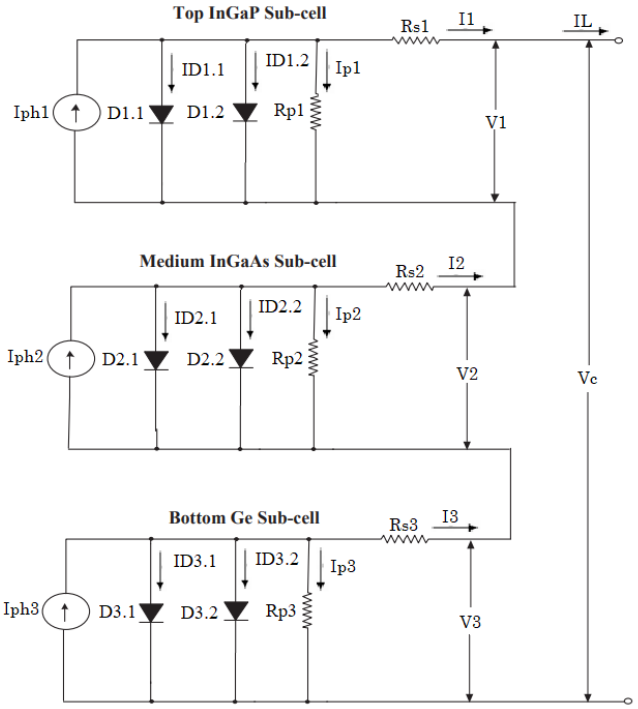

Figure 2-17 Equivalent circuit for double diode TJSC model

The I–V relationship for each sub cell is determined by ignoring the effects of the reverse branch (due to the uniform illumination) and the shunt resistance.

The ideality factors are fixed at values of 1 and 2 in this form of the two-diode model, and The dark saturation currents, which are temperature dependent, are as follow:

$$I_{Si.1} = k_{i.1} \times T^3 \times e^{\frac{-E_{gi}}{KT}} \tag{2.18}$$

$$I_{Si.2} = k_{i.2} \times T^{\frac{3}{2}} \times e^{\frac{-q \times E_{gi}}{2KT}} \tag{2.19}$$

Where $k_{i.1}$ and $k_{i.2}$ are constants. Contrary to the model of a single diode, the voltage in this case is not an explicit function of the current and must be extracted iteratively. The two-diode model has seven empirical parameters that must be calibrated against experimentally measured data, including $k_{i.1}$, $k_{i.2}$, and R_S. The only resistance that must be identified is the single lumped series resistance, as the serial voltage drop in the circuit is simply the sum of the effects of the three distinct resistors: $I_i(R_{s1} + R_{s2} + R_{s2}) = I_i R_s$, as deduced from Fig. 2-17 [26].

2.4.3 Improvements of TJSC

One of the most significant improvements in triple junction solar cells is the use of new materials with improved bandgap energies, such as gallium arsenide (GaAs) and indium gallium phosphide (InGaP). In a study by **Hossain et al (2021)[27]**, a triple junction solar cell using InGaP as the top subcell, GaAs as the middle subcell, and silicon (Si) as the bottom subcell achieved a high conversion efficiency of 33.3%. This was attributed to the improved absorption of light by the InGaP and GaAs subcells, as well as reduced recombination losses due to the use of tunnel junctions. Another study where **Kikuo Makita et all (2019)[28]** , fabricated an InGaP/AlGaAs//Si three-junction solar cell using smart stack technology that refers to the use of advanced multilayer structures or stacks of different materials to enhance the performance and efficiency of solar cells , achieving a maximum efficiency of 30.8% at 1 sun. The high efficiency was achieved by optimizing the upper GaAs-based cell (InGaP/AlGaAs two-junction cell) and employing a tunnel oxide passivated contact (TOPCon) Si cell.

Another approach to improving triple junction solar cells is the use of antireflective coatings (ARCs) to reduce reflection losses. In a study by **Ram Homier et all (2012)[29],** presented a simulation performance of a SiO2 /LFSiN ARC for III– V/Ge 3JSCs using real material optical properties. This ARC is effective in minimizing the reflection losses over the wavelength range of the limiting subcell for both top and middle subcell-limited triple-junction solar cells. The simulation results indicate that the ARC maintains its performance even when subjected to variations in the parameters of the plasma-enhanced chemical vapor deposition (PECVD) films, such as thickness and refractive index. Overall, The study suggests that SixNy, a low-absorption material deposited using low-frequency PECVD, can serve as a versatile coating for multijunction solar cells. Apart from its anti-reflective properties, it also has the potential for surface passivation and encapsulation. The PECVD technique, widely used in the silicon solar cell industry, offers the advantage of cost-effectively depositing thin films on a large scale.

Triple junction solar cells can also benefit from novel device architectures, such as the use of nanowires to improve light absorption and carrier collection. In a study by **Tian et al. (2019)[30],** a triple junction solar cell using nanowires made of InGaAsP/InP was developed. The nanowires acted as both light absorbers and carrier collectors, resulting in improved light trapping and reduced recombination losses. This led to a record-high conversion efficiency of 35.9% for a triple junction solar cell.

2.5 Conclusion

In conclusion, this chapter has provided a comprehensive explanation of the Single, Dual and Triple junction solar cells, giving details about their electrical circuits and the a few types of material combination from different studies that achieved a certain result and efficiency, also this chapter went deep into Triple junction solar cells and demonstrates the equations needed on the modeling process alongside a state of art to finish with, because it’s our main subject.

Overall, this chapter is a starting point to dive into the modeling part, which is going to be discussed in the next chapter.

CHAPTER 3.

PARAMETERS IDENTIFICATION OF TJSC

3.1 Introduction

This chapter focuses on a particular method for extracting electrical parameters from triple junction solar cells. Important parameters such as open-circuit voltage, short-circuit current, fill factor, and series resistance can be determined using this method. By employing this method to several triple junction cell configurations, we hope to assess its efficacy and applicability across various kinds of designs. in addition, we recognize the difficulties associated with modeling triple junction solar cells, such as the need to account for material properties, layer thicknesses, and interfaces. To ensure accurate parameter extraction and improve our comprehension of the performance of devices under diverse operating conditions, it is essential to overcome these obstacles.

The first goal of this chapter is to provide the particular approach for parameter extraction in triple junction solar cells, examining its underlying concepts and mathematical formulations. Second, we will apply this approach to a variety of triple junction cell designs, analyze the results, and assess the method's dependability and adaptability, we hope that by accomplishing these goals, we will be able to make a significant contribution to the development of modeling tools for triple junction solar cells and give useful insights into the electrical parameters and performance characteristics of these complicated devices. In the end, the purpose of this research is to make it easier to build and optimize triple junction solar cells in order to generate more energy in a sustainable manner and achieve higher levels of efficiency.

3.2 Proposed method for parameters extraction

In this part we used the proposed method by **S. Chtita and all [31],** where they presented a new method to model a photovoltaic panel that uses a triple junction cell for a nanosatellite application. The suggested model is based on a simplified single-diode (4-parameter) electrical circuit, and these parameters are retrieved while taking into account the effects of environmental parameters such as irradiance and temperature equivalent to the sun spectrum outside the AM0 atmosphere (T=28°; G=1350 W/m²).

For this, the NanoPower P110-A solar panel from GOMspace in Fig. 3-1 is chosen. This module is made up of two AZURSPACE's InGaP / GaAs / Ge 3G30A cells connected in series and providing an effective surface of 63.36 cm2 and an output voltage at 4.2 V [32].

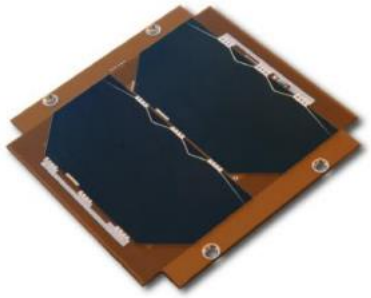

Figure 3-1 NanoPower P110-A solar panel equipped with 2 PV cells type 3G30A.

These are the electrical parameters of the PV cells type 3G30A:[31]

1 cell 30.18 cm2 – BOL – AM0 spectrum (1350 W/m2 - 28 °C)		
Parameter	Value	Description
Voc	2690 mV	Average open circuit voltage
Isc	519.6 mA	Average short circuit current
Vm	2409 mV	Voltage at MPP
Im	502.9 mA	Current at MPP
Pmax	1.211 W	Maximum power
η	29.3 %	Average efficiency
∂VoC/∂T (Kv)	-6.2 mV/°C	Temperature gradient of Voc
∂IsC/∂T (Ki)	0.36 mA/°C	Temperature gradient of Isc
∂VOPT/∂T	-6.7 mV/°C	Temperature gradient of Vm
∂IOPT/∂T	0.24 mA/°C	Temperature gradient of Im

Table 2 electrical characteristics of the PV cells type 3G30A

3.2.1 The mathematical method

To model this solar cell a simplified model has been used, It includes a current source, a diode, the series resistance, and the shunt resistance, the figure bellow show the simplified electrical circuit [31]

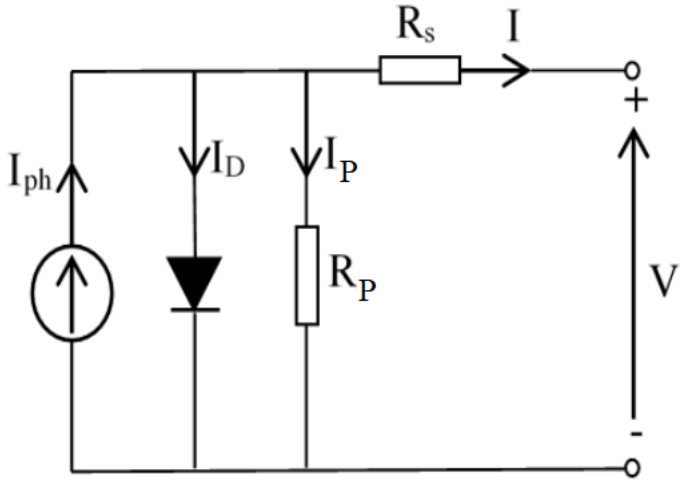

Figure 3-2 Simplified equivalent circuit of the PV cell

The photovoltaic module's electrical behavior is connected to I_{ph}, I_{rs}, R_s, n, and R_P, as well as two other environmental parameters, temperature and solar irradiation.

The modeling of the photovoltaic module necessitates the extraction of I_{ph}, I_{rs}, R_s, n, and R_P, which is accomplished through the use of a mathematical method with the main goal of determining the unknown parametersI_{ph}, I_{rs}, R_s, R_P, n of the single-diode model. We need at least five equations to obtain these values, first here's the output current equation of the simplified model knowing that R_P is neglected in this model:

$$I = I_{ph} - I_S\left(e^{\frac{q(V+IR_S)}{N_S nKT}} - 1\right) \quad (3.1)$$

Where N_s is the number of cells in series and n is the ideality factor.[31]

I_{ph} (photocurrent) can be simply calculated, and this current varies with irradiance and temperature.

$$I_{ph} = (I_{sc} + K_i(T - T_r))\frac{G}{G_r} \tag{3.2}$$

And here is the equation of the reverse saturation current I_s that contain two unknowns

$$I_s = I_{rs} \times \left(\frac{T}{T_r}\right)^3 \times e^{\left\{\frac{qE_{g0}}{n.k}\left(\frac{1}{T_r}-\frac{1}{T}\right)\right\}} \tag{3.3}$$

I_{rs} and n:

Following that, the number of unknown parameters is now limited to four (I_{rs}, R_s, R_P, n). The suggested approach consists of two steps for determining these parameters. First, the shunt resistance Rsh is ignored as we mentioned earlier.

The second step is to apply the manufacturer's characteristic equations for the three spots (0, I_{sc}), (V_{oc}, 0), and (V_m, I_m) under standard spatial test conditions (STCs: AM = 0, Gr =1350 W/m2, T = 28 °C) and replace them in the output current equation. [31]

Now we'll put: $A = \frac{q}{N_s.n.KT}$

Following the mathematical calculations, the parameters are extracted using the following equations:

$$I_{rs} = \frac{I_{sc}}{\exp(AV_{oc}) - \exp(AI_{sc}R_s)} \tag{3.4}$$

$$\frac{I_{sc}}{\exp(AV_{oc}) - \exp(AI_{sc}R_s)} = \frac{I_m}{\exp(AV_{oc}) - \exp[A(V_m + R_sI_m)]} \tag{3.5}$$

$$\frac{I_m}{\exp(AV_{oc}) - \exp[A(V_m + R_s I_m)]} = \frac{\frac{I_m}{V_m - R_s I_m}}{A\exp[A(V_m + R_s I_m)]} \quad (3.6)$$

The methodology adopted for the proposed method is presented in the flowchart:[31]

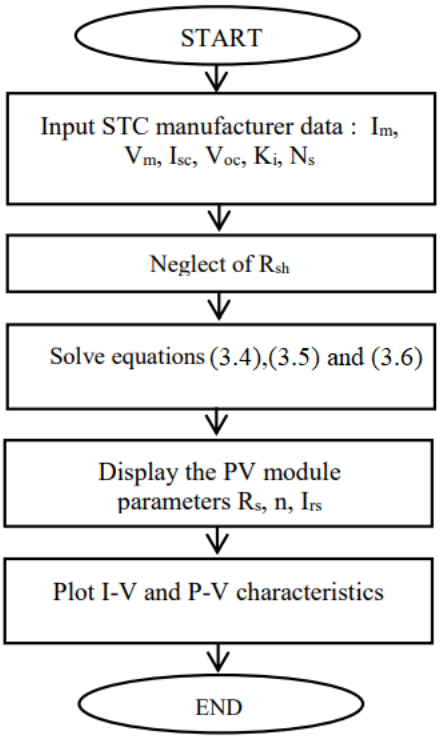

Figure 3-3 Flowchart of the proposed extraction method

The previous equations were solved using MATLAB and the results are in the following table :

Parameters	NanoPower P110-A (GOMspace)
$R_s[\Omega]$	0.0269
n	3.0738
$I_{rs}[A]$	1.769×10^{-15}

Table 3 extracted parameters of NanoPower P110-A using MATLAB

Then, the corresponding I-V and P-V curves are plotted under standard spatial test conditions (STC space: AM = 0, Gr = 1350 W/m2 , T = 28 °C) in order to compare them with the manufacturer data :

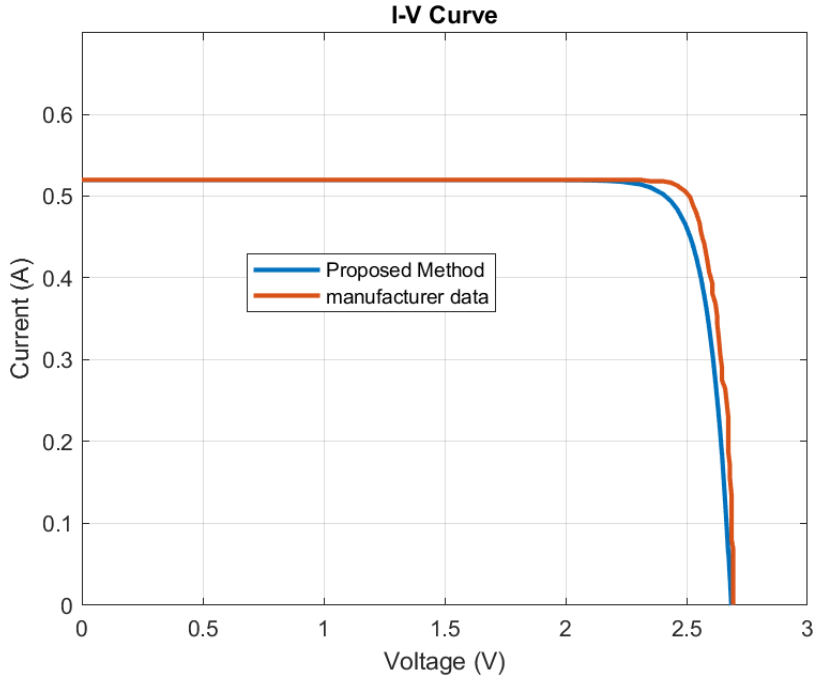

Figure 3-4 Comparison of the I-V characteristics of the proposed method and manufacturer data at STC (space)

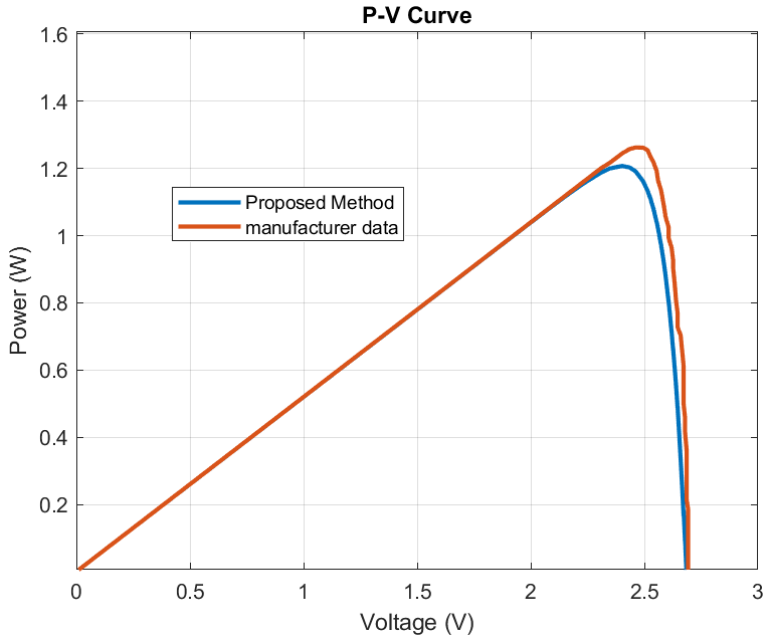

Figure 3-5 Comparison of the I-V characteristics of the proposed method and manufacturer data at STC (space)

Figures (3-4, 3-5) illustrates the curves derived by the suggested method and those provided by manufacturer data. As shown in the pictures, both curves are almost identical, also, the maximum power at the P-V curves almost achieve the same MPP with a little error, demonstrating that the suggested method is very precise for this type of panel.

We have also calculated the Root Mean Squared Error (RMSE) between the proposed method and the data points, it is frequently used to evaluate a prediction model's overall accuracy.

It benefits from being expressed in the same units as the real and anticipated values, which makes it easier to comprehend. The results are in the table below:

	I-V curve	P-V curve
RMSE	0.063687	0.16891

Table 4 RMSE of I-V and P-V curves of NanoPower P110-A

Prediction Depending on the curves and the error calculation, it’s obvious that the error in the I-V curve is smaller than the error in the P-V curve, but we can still say that the method is accurate because the error is small.

3.2.2 The effect of irradiance

The I-V and P-V characteristics of the GOMspace NanoPower P110-A Photovoltaic Module are shown in Figures 7 and 8 for irradiation levels of 0.25*Gr, 0.5*Gr, 0.75*Gr, and Gr at a reference temperature Tr=28°C.

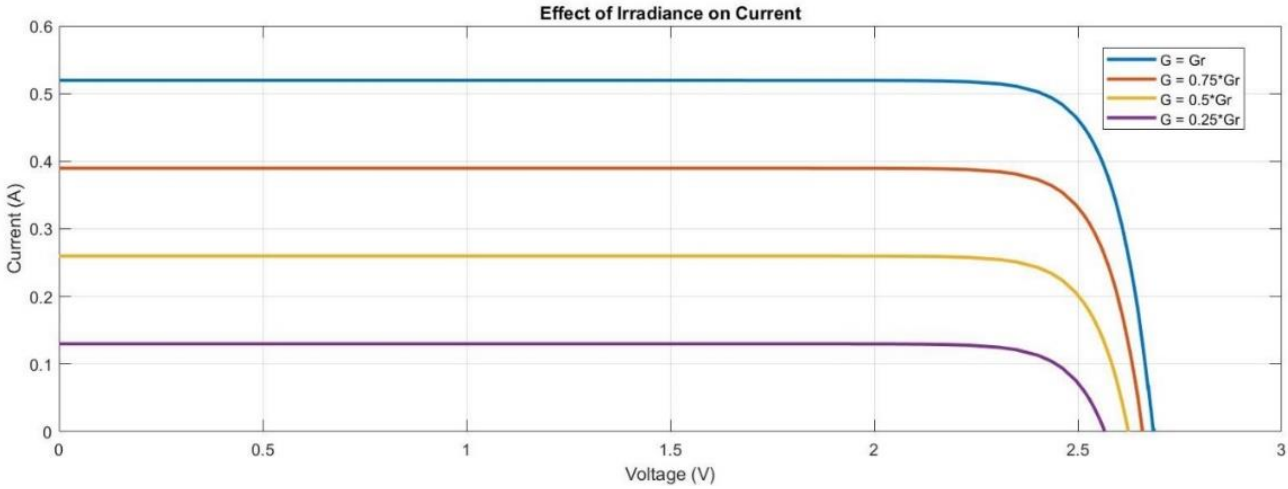

Figure 3-6 The effect of irradiance on the I-V curve

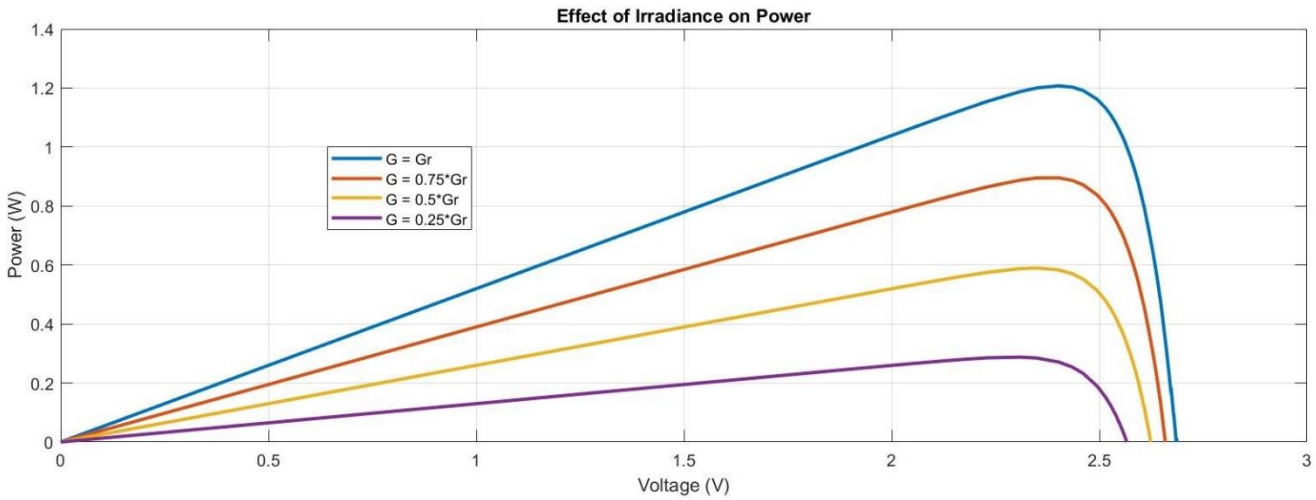

Figure 3-7 The effect of irradiance on the P-V curve

According to Figs. 3-6 and 3-7, the short-circuit current Isc of the solar module varies with irradiance. When the irradiation increases, the output current increases significantly, while the voltage increases a little, because the short-circuit current Isc is a linear function of the irradiation, whereas the open circuit voltage Voc is a logarithmic function that works on causing a clear increase in the photovoltaic module's power output.

3.2.3 The effect of temperature

In this part, a demonstration of the effect of temperature change on the I-V and P-V curves done.

After the variation of the temperature from T=90°C, T=10°C, T=-50°C and with a reference temperature and irradiance Tr=28°C, Gr=1350W/m², we got the following results:

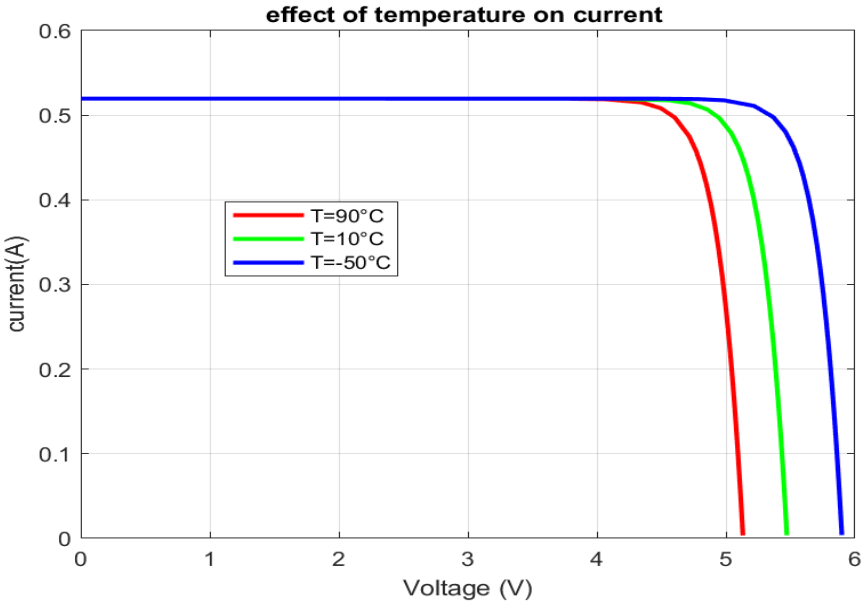

Figure 3-8 the effect of temperature on the I-V curve

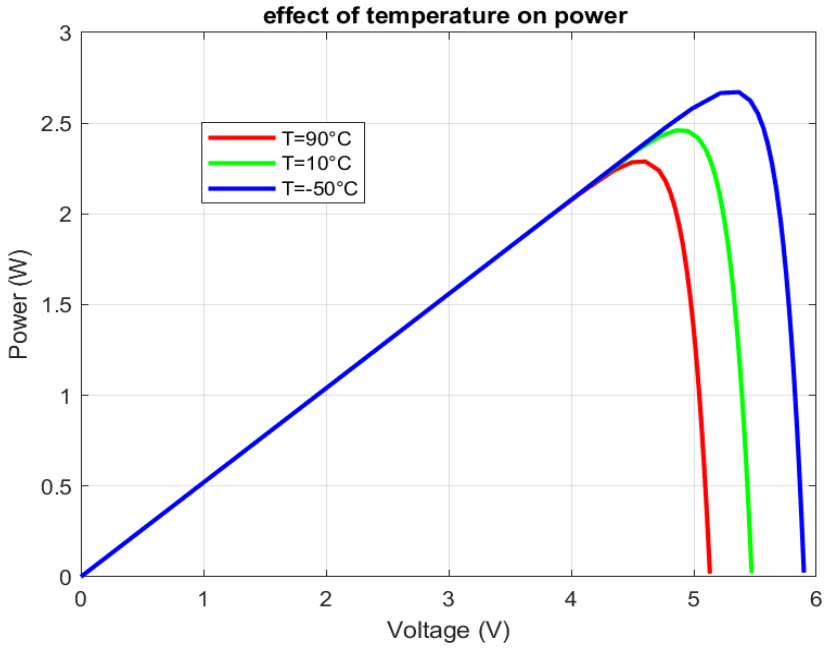

Figure 3-9 the effect of temperature on the P-V curve

From these results, it is evident that the open circuit voltage Voc of the module is temperature dependent, as the operating temperature of the module rises, the output voltage decreases, resulting in a decrease in the photovoltaic module's output power. We should point that the temperature change also affect the short circuit of the module but the effect is negligible compared to the huge variation in the voltage.

3.3 Validation of The Proposed Method

3.3.1 TJSC based on GaInP, GaAs and Ge junction

The proposed method is performed on another type of TJSC, which means different characteristics, to do this we based our test on the work of **A. Hadjdida Et Al [24] .**The purpose of their body work was conduct to an analytical modeling, simulation, and comparative study on the efficiency of multi-junction solar cells. The results of this research will be utilized in the design of photovoltaic technologies with high conversion efficiencies, applicable both on Earth and in space.

Firstly, we will take the electrical parameters of the cell they worked on:

The electrical parameters of the cell	InGaP/GaAs/Ge
Voc (V)	2.6902
Isc (mA/cm²)	16.5210
Vm (V)	2.5550
Im (mA/cm²)	16.0908
Pm (W)	0.411226
FF (%)	92.5333

Table 5 electrical parameters of an InGaP/GaAs/Ge solar cell

Then we will apply the proposed method to extract the unknown's parameters I_{rs}, R_s, n

The results are in the table below:

Parameters	A. Hadjdida Et Al. cell
$R_s[\Omega]$	0.078645
n	2.768
$I_{rs}[A]$	9.0448×10^{-18}

Table 6 the extracted parameters the InGaP/GaAs/Ge solar cell using the proposed method

Now we will plot both our method results and the results of A. Hadjdida Et Al and calculate the error between the 2 curves:

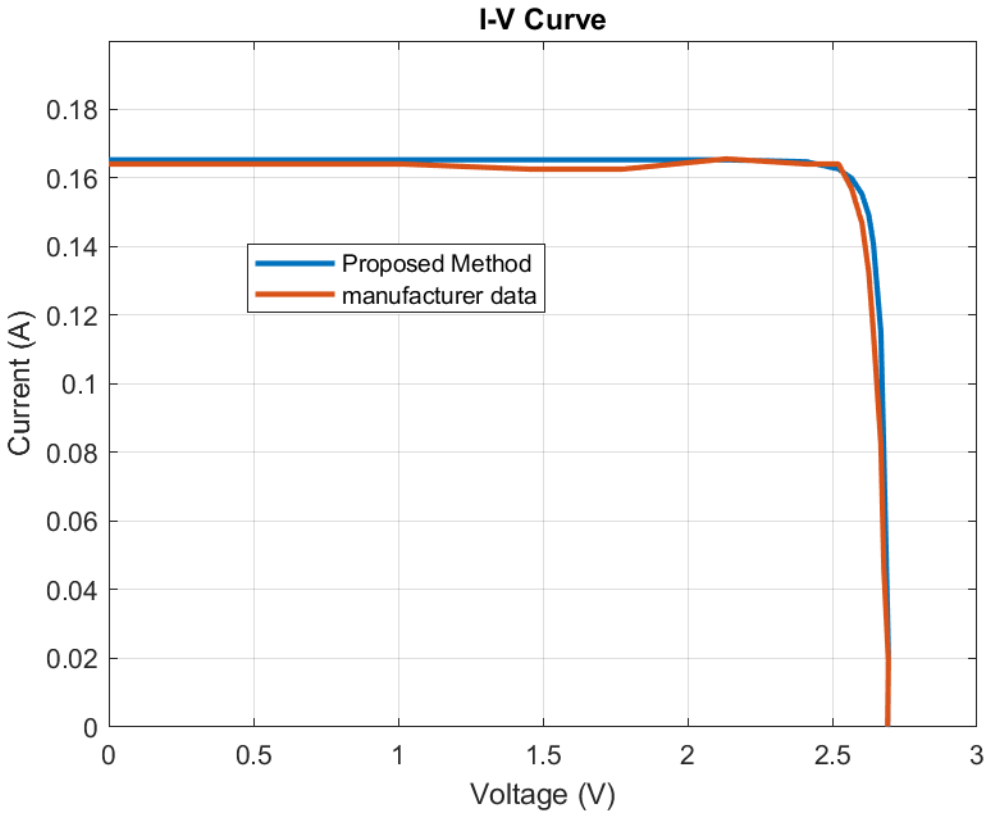

Figure 3-10 Comparison of the I-V characteristics of the proposed method and manufacturer data of InGaP/GaAs/Ge solar cell

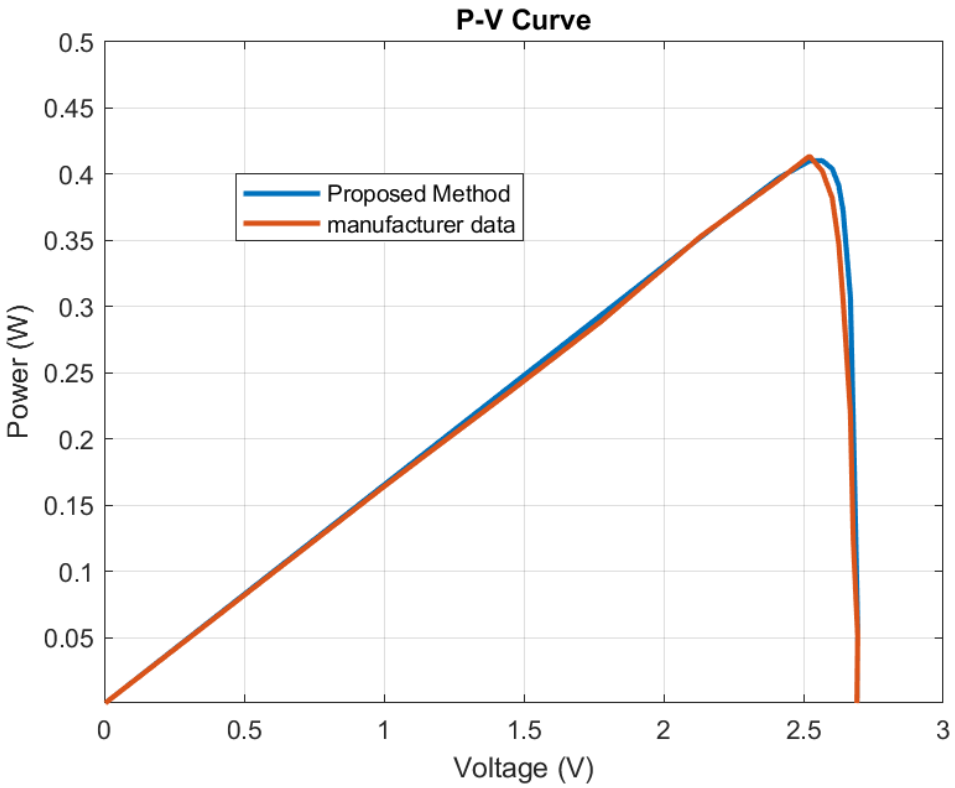

Figure 3-11 Comparison of the P-V characteristics of the proposed method and manufacturer data of InGaP/GaAs/Ge solar cell

As we said earlier, now we will calculate the Root Mean Squared Error (RMSE) between the proposed method and the data points:

	I-V curve	P-V curve
RMSE	0.013442	0.035675

Table 7 RMSE of I-V and P-V curves of the InGaP/GaAs/Ge solar cell

We can see that we got even better results than the previous calculations, the error is very small and the I-V and P-V curves are nearly similar, so once again, the proposed method for parameters extraction is reliable, and gives satisfying results.

3.3.2 TJSC based on C3MJ+ triple-junction (InGaP/InGaAs/Ge)

To assure that the proposed method is reliable in different TJSC, we used it to extract the parameters in another work by **Anaty, M et al[33]** ,A method to modeling a C3MJ+ solar cell utilizing a single diode equivalent circuit model for triple-junction has been proposed by them in the study, the modeling was carried out with the help of Matlab/Simulink software.

We will repeat the same steps, first we need the manufactures electrical parameters:

The electrical parameters of the cell	InGaP/GaAs/Ge
Voc (V)	3.21
Isc (A/m²)	0.719
Vm (V)	2.87
Im (A/m²)	0.683
Pm (W)	1.96
FF (%)	84.95

Table 8 electrical parameters of a C3MJ+ triple-junction

Using the proposed method to extract the parameters I_{rs}, R_s, n is the next step, after entering the electrical parameters into our MATLAB code, the results are as follow:

Parameters	Anaty, M et al cell
$R_s[\Omega]$	0.019639
n	2.0337
$I_{rs}[A]$	1.1287×10^{-9}

Table 9 the extracted parameters from Anaty, M et al cell using the proposed method

Next step is to draw both curves and calculate the RMSE between them

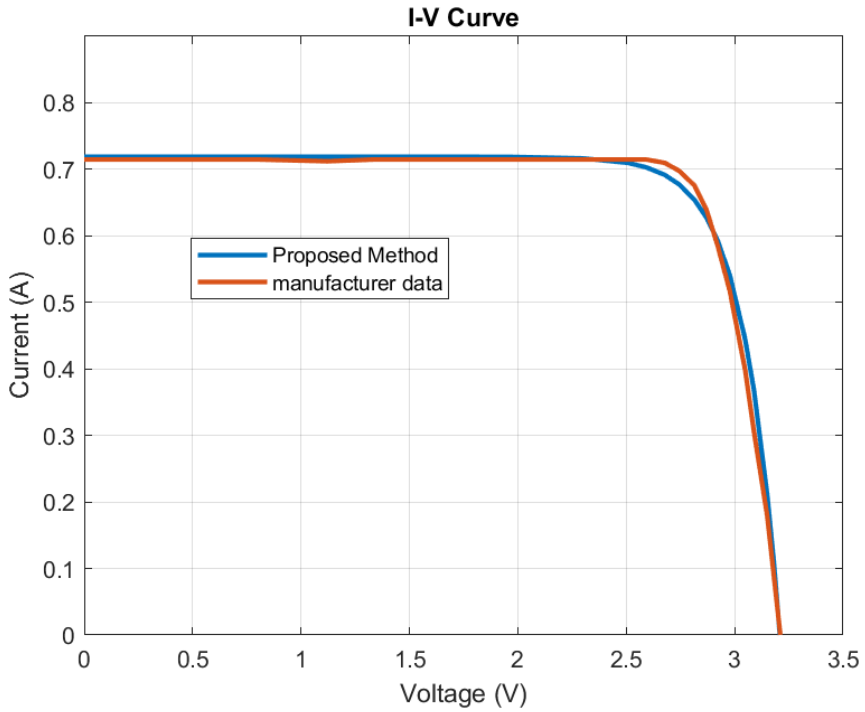

Figure 3-12 Comparison of the I-V characteristics of the proposed method and manufacturer data of C3MJ+

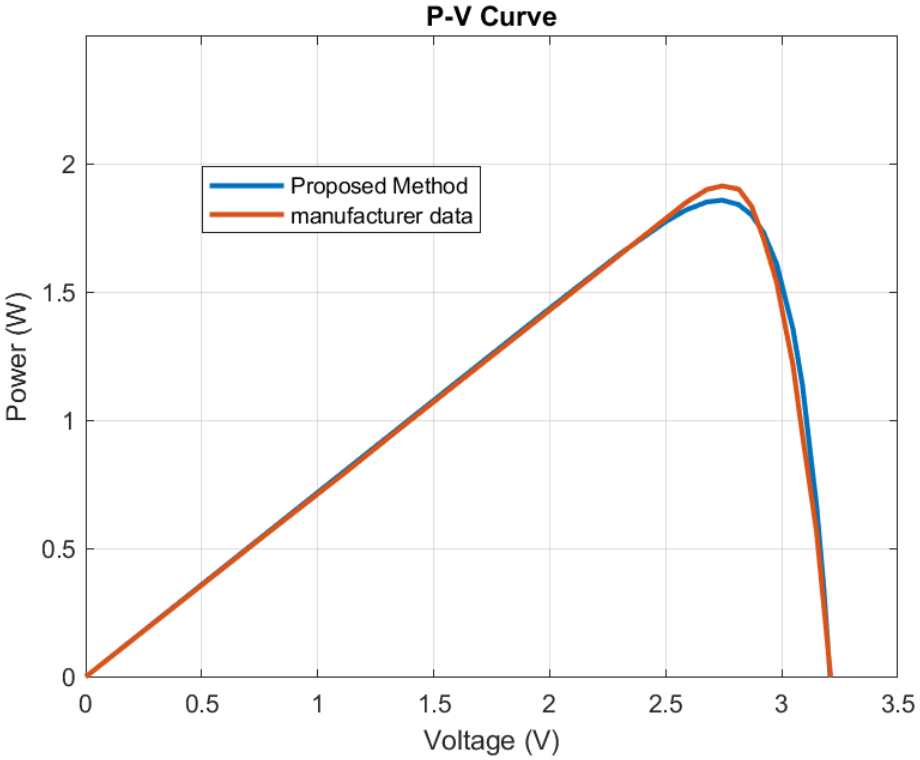

Figure 3-13 Comparison of the P-V characteristics of the proposed method and manufacturer data of C3MJ+

Last step is to calculate the Root Mean Squared Error:

	I-V curve	P-V curve
RMSE	0.021192	0.063821

Table 10 RMSE of I-V and P-V curves of C3MJ+

For the third time we can remarque the tiny error between the data point and the proposed method so we can say that the proposed method can be applied on different cells with different electrical parameters, giving us as a result a satisfying I-V curve and a pleasing outcome.

3.4 Physical model simulation in SIMULINK

The figure below shows the designed physical model based on the previous work of **S. Chtita et all[31]**, using the NanoPower P110-A solar panel equipped with 2 PV cells type 3G30A.

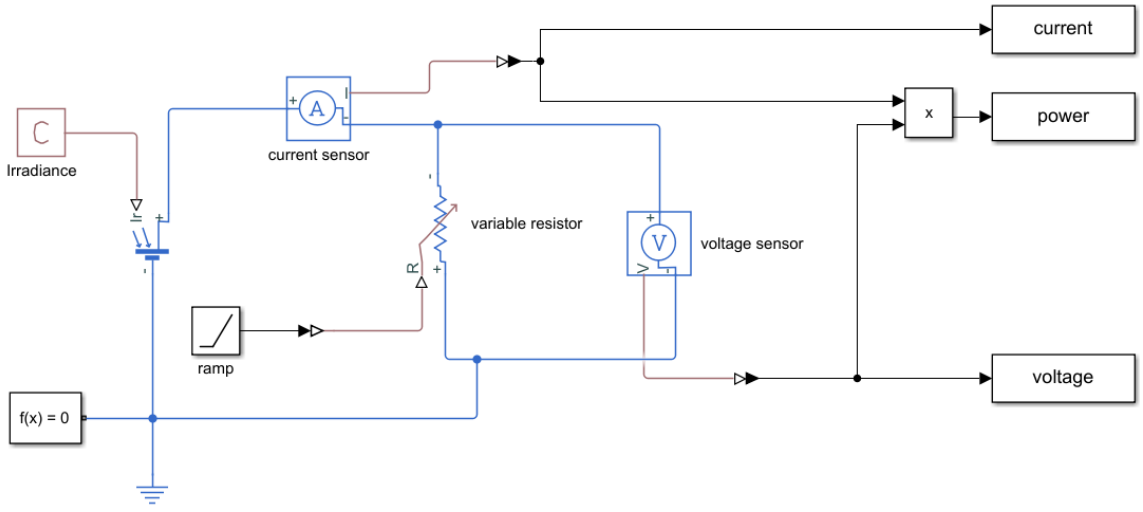

Figure 3-14 the physical of the cell model using Simulink

After entering the electrical parameters to the physical model solar cell, we just simulate and the all data of current, voltage and power go to workspace in MATLAB, then we plot the I-V and P-V curves and compare them with the actual proposed method.

Here is the I-V and P-V curves using a physical model:

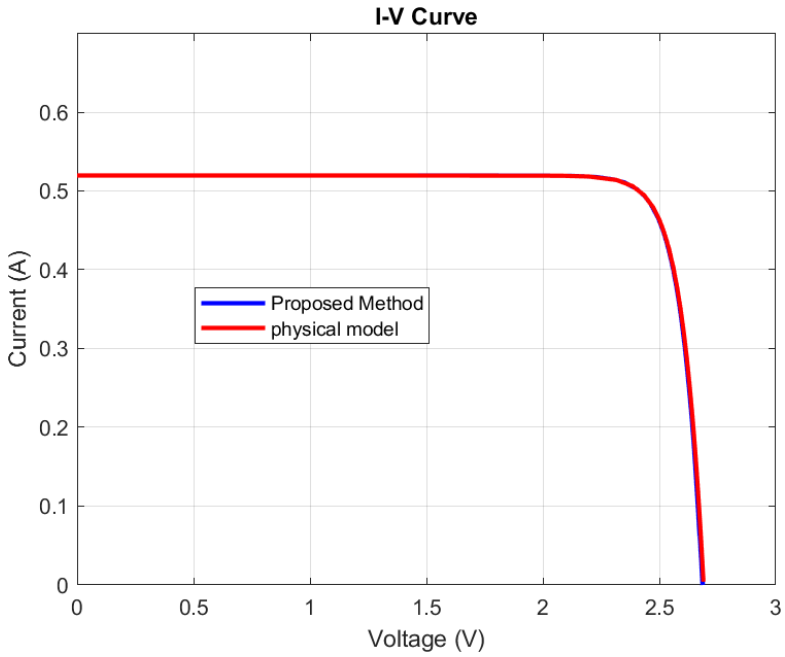

Figure 3-15 I-V curve of the physical model compared to the proposed method curve

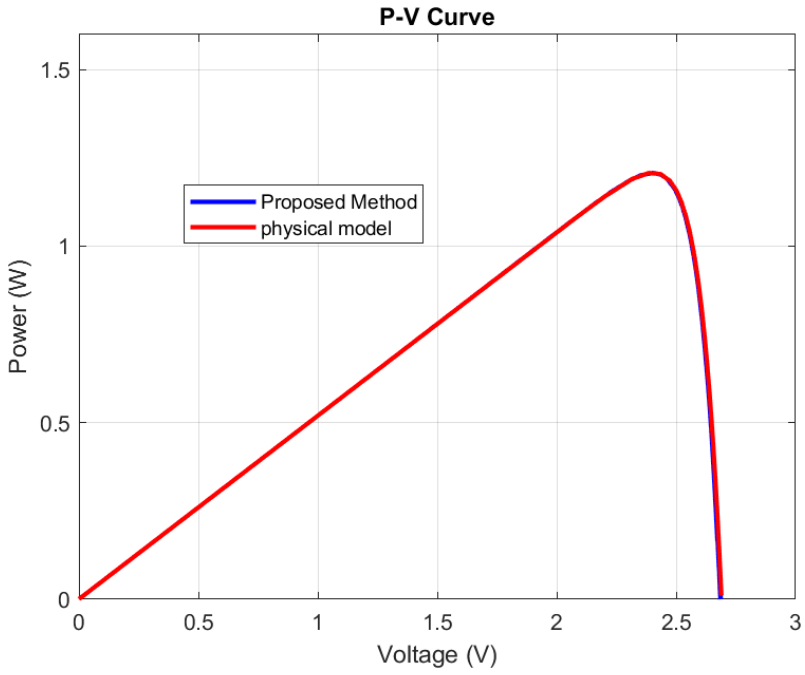

Figure 3-16 I-V curve of the physical model compared to the proposed method curve

The results are satisfying and identical to the proposed method curve plotted earlier, which once more make the proposed method more solid and reliable.

3.5 Conclusion

This chapter discussed and described a chosen method that we used in order to extract the PV cell unknown parameters , we first modelized the IV characteristics of the cell and the effect of the temperature and irradiance variation , then a test of the proposed method was done in order to expand our study field to multiple cells , the results were really satisfying and the method that we chose to extract these parameters was validated , last thing we did was trying a physical model simulation using the parameters that we extracted and the results were identical to the analytical work .

Overall, our work was based on verifying and validating an analytical model to get the parameters of a TJSC, which was successfully achieved by showing a good performance and this method is solid and can be used to model different types of triple junction solar cells.

GENERAL CONCLUSION

As the last touches are being put on our thesis , we can say that the research conducted in this dissertation has contributed to the existing knowledge of aerospace photovoltaic systems, according to the findings of the study, temperature, radiation, and efficiency are the three most important aspects that play a role in determining how well solar panels function in space, the research has also offered new models and methodologies for optimizing the design of solar cells, which can increase their performance and dependability in space.

The results of our work were very satisfying and we came up in the end that the proposed method for parameters extracting can be used to model different types of Triple Junction Solar Cells, the method showed a great performance compared to other cells and from that it can be reliable and very applicable to model the nanosatellite PV cells.

Based on the great results of our work, we confidently affirm that our fundamental objective, diligently pursued with steadfast determination, has without a doubt been completed successfully. The potent integration of the method that we used paved the way for many upcoming experiments in this field.

The validity and effectiveness of the suggested strategy unmistakably demonstrate the exceptional success we have attained as a result of our efforts. Thus, fueled by the spirit of innovation and commitment to excellence, we proudly declare the resounding success of our research.

REFERENCES

[1] https://www.space.com/24839-satellites.html#section-brief-history-of-artificial-satellites

[2] European Space Agency, ENABLING & SUPPORT, Types of orbits.

[3] Dan Stillman, Institute for Global Environmental Strategies , NASA Knows! , What Is a Satellite?

[4] https://rps.nasa.gov/news/35/what-powers-a-spacecraft/

[5] Amina, S.M.S. and B.A. djamila, mémoire"Dimensionnement d'une installation photovoltaique". 2015.

[6] Basic Photovoltaic Principles and Methods, Technical Information Office, Solar Energy Research Institute.1982

[7] CASSORE, F., G. ORLANDI, and M. RAU, cellules photovoltaïques a colorant .

[8] Photovoltaic design and installation for dummies , Ryan Mayfield , President, Renewable Energy Associates

[9] Rooftop Solar PV System Designers and Installers Training Curriculum d By Andre Susanto , Chitra Priambodo , Castlerock Consulting .2015

[10] https://www.energy.gov/eere/solar/multijunction-iii-v-photovoltaics-research

[11] https://www.energy.gov/eere/solar/organic-photovoltaics-research

[12] https://www.alternative-energy-tutorials.com/photovoltaics/solar-cell-i-v-characteristic.html

[13] Basic Characteristics and Characterization of Solar Cells (2018).

[14]"Silicon Solar Cells" by Martin A. Green

[15] Chowdhury, Sanchari & Kumar, Mallem & Dutta, Subhajit & Park, Jinsu & Kim, Jaemin & Kim, Seyoun & Ju, Minkyu & Kim, Youngkuk & Cho, Young & Cho, Eunchel & Yi, Junsin.

(2019). High-efficiency Crystalline Silicon Solar Cells: A Review. New & Renewable Energy. 15. 36-45. 10.7849/ksnre.2019.3.15.3.036.

[16] Tamrakar, V., Gupta, S. C., & Sawle, Y. (2015). Study of characteristics of single and double diode electrical equivalent circuit models of solar PV module. 2015 International Conference on Energy Systems and Applications.

[17] Fang, J., Ren, Q., Wang, F., Wei, C., Yan, B., Zhao, Y., & Zhang, X. (2018). Amorphous silicon/crystal silicon heterojunction double-junction tandem solar cell with open-circuit voltage above 1.5 V and high short-circuit current density. Solar Energy Materials and Solar Cells, 185, 307–311.

[18] Alshkeili, S., & Emziane, M. (2013). Design of Si/Ge Dual Junction Solar Cell Devices. Energy Procedia, 42, 698–707.

[19] Ataser, T., Akin Sonmez, N., Ozen, Y., Ozdemir, V., Zeybek, O., & Ozcelik, S. (2018). Developing of dual junction GaInP/GaAs solar cell devices: effects of different metal contacts. Optical and Quantum Electronics, 50(7).

[20] Yang, Terry. (2010). 46% Efficient Split Spectrum Cells Project - Tandem Cell Spectral Response Characterisation.

[21] Hegazy Rezk , El-Sayed Hasaneen (2015) , A new MATLAB/Simulink model of triple-junction solar cell and MPPT based on artificial neural networks for photovoltaic energy systems .

[22] A.HadjDida , M.Bekhti (2017) , Study Modeling and Simulation of the Electrical Characteristics of Space Satellite Solar Cells

[23] Khaled Teffah , Youtong Zhang , "Modeling and experimental research of hybrid PV-thermoelectric system for high concentrated solar energy conversion ",Solar Energy Vol 157, Pages 10-1915 , November 2017

[24] A. Hadjdida Et Al. , "Analytical Modelling, Simulation and Comparative Study of Multi-Junction Solar Cells Efficiency," INTERNATIONAL JOURNAL OF RENEWABLE ENERGY RESEARCH , vol.8, no.4, pp.1824-1832, 2018

[25] Gideon Segev, Gur Mittelman, and Abraham Kribus, "Equivalent circuit models for triple junction concentrator solar cells," Solar Energy Materials and Solar Cells, vol. 98, pp. 57-65, March 2012.

[26] Segev, G., Mittelman, G., & Kribus, A. (2012). Equivalent circuit models for triple-junction concentrator solar cells. Solar Energy Materials and Solar Cells, 98, 57–65.

[27] Hossain, M. A., Wu, J., Zhang, X., Wang, W., Ye, H., & Wong, W. (2021). InGaP/GaAs/Si triple junction solar cells with high conversion efficiency of 33.3%. Solar Energy.

[28] Kikuo Makita ,Hidenori Mizuno , Takeshi Tayagaki , Taketo Aihara ,Ryuji Oshima , Yasushi Shoji , Hitoshi Sai , Hidetaka Takato , Ralph Müller ,Paul Beutel , David Lackner , Jan Benick , Martin Hermle , Frank Dimroth ,Takeyoshi Sugaya (2019) .III-V//Si multijunction solar cells with 30% efficiency using smart stack technology with Pd nanoparticle array .

[29] Ram Homier Abdelatif Jaouad, Artur Turala, Christopher E. Valdivia, Denis Masson, Steven G. Wallace, Simon Fafard, Richard Ares, and Vincent Aimez (2012) , Antireflection Coating Design for Triple-Junction III–V/Ge High-Efficiency Solar Cells Using Low Absorption PECVD Silicon Nitride . IEEE JOURNAL OF PHOTOVOLTAICS

[30] Tian, W., Cao, X., Li, X., Chen, K., Zhang, C., & Chen, L. (2019). InGaAsP/InP nanowire array solar cells with high efficiency for triple-junction solar cells. Journal of Alloys and Compounds.

[31] S. Chtita, Y. Chaibi, A. Derouich and J. Belkadid, "Modeling and Simulation of a Photovoltaic Panel Based on a Triple Junction Cells for a Nanosatellite," 2018 International Symposium on Advanced Electrical and Communication Technologies (ISAECT), Rabat, Morocco, 2018, pp. 1-6, doi: 10.1109/ISAECT.2018.8618840.

[32] “GOMspace | P110 Solar Panel”, Datasheet

https://gomspace.com/UserFiles/Subsystems/datasheet/gs-ds-nanopower-p110-210.pdf

[33] Anaty, M. K., Belkasmi, M., Bouziane, K., Aggour, M., & El Ouahabi, M. (2016). Modeling and simulation of a C3MJ+ triple junction solar cell using Matlab/Simulink. 2016 International Renewable and Sustainable Energy Conference (IRSEC).